2024

# Analysis of the Immune Response After Readministration of a Novel AAV6 Gene Therapy Containing TLR9 Inhibitory Sequences

Sarah Allen
*Medical University of South Carolina*

Analysis of the Immune Response After Readministration of a Novel AAV6 Gene Therapy Containing TLR9 Inhibitory Sequences by

Sarah Elysse Allen

A thesis submitted to the faculty of the Medical University of South Carolina in partial fulfillment of the requirements for the degree of Master's in Biomedical Sciences in the College of Graduate Studies

Department of Molecular and Cellular Biology and Pathobiology

2024

Approved by:

Chairman, _____
Martin Kang

_____
John Baatz

_____
Kris Helke

_____
Jeffery Jones

_____
Catrina Robinson

# Table of Contents

List of Figures..... v

Abbreviations.....vi

Abstract.....vii

1.0 Introduction.....1

1.1 Surfactant Protein-B.....1

1.2 Surfactant Protein-B deficiency.....1

1.3 Use of adeno-associated virus (AAV) for a gene therapy treatment.....2

1.4 The role of the TLR9 pathway in the regulation of the innate and adaptive immune system.....3

1.5 TLR9 inhibition and its reduction in the inflammatory and immune response to AAV.....9

1.6 Redosing of AAV using TLR9 inhibition.....5

2.0 Materials & Methods.....9

2.1 Bacterial transformation of *E. coli*.....9

2.2 Plasmid Purification.....10

2.2.1 Mini Prep.....10

2.2.2 DNA gel electrophoresis.....11

2.2.3 Maxi prep for plasmid purification.....11

2.2.4 AAV Production and Purification.....13

2.3 Animal Model.....14

2.4 AAV Administration.....15

2.4.1 Anesthesia by intraperitoneal injection of Ketamine/Xylazine.....15

2.4.2 Subcutaneous injection of saline……..….15

2.4.3 Intubation and Endotracheal delivery of AAV……..…..….15

2.5 RNA Extraction for gene expression analysis……..…17

2.6 Gene expression analysis……..18

2.7 qPCR validation of genes from gene expression analysis……....….18

2.8 Protein isolation of murine lung tissue for validation experiments…...19

2.9 Bradford assay of murine lung homogenate…….…....20

2.10 Western blotting…….……...…20

2.10.1 ProSP-B…….……..……..23

2.10.2 Mature SP-B ……..……..23

2.10.3 Tbx21 ……..…….…...23

2.10.4 Stat1 ……..……....24

2.10.5 GAPDH…..……..……..…..24

2.10.6 Vinculin……...……..25

2.10.7 Histone H3……....…25

2.11 Serum Collection by saphenous vein bleeds……....25

2.12 Serum antibody levels by ELISA…….26

2.13 AMI-HT Imaging…….28

2.14 ROI quantification……28

2.15 Western blot quantification……..…29

2.16 Statistical analysis…….29

3.0 Results……..…….29

3.1 Vector Production and Generation……...……29

3.2 Vector assessment study……...35

3.3 TLR9i sequences improve human *SFTPB* expression in repeat doses……...41

3.4 Gene expression analysis……..…44

3.5 Validation of gene expression analysis ……..…..52

3.6 Validation of *Stat1* by immunoblotting……..55

3.7 Validation of *Tbx21* by immunoblotting……59

4.0 Discussion…….…….…62

4.1 Assessment of AAV Vector Efficacy……..…62

4.2 Gene expression analysis……..63

5.0 Conclusion and Future Directions……..……..……64

6.0 References……...…66

## List of Figures


| Figure Title Number | Figure | Page Number |
|---|---|---|
| 1 | Schematic of the TLR9 pathway recognition of unmethylated CpG DNA motifs | 4 |
| 2 | Contents of AAV6.2FF vector with and without TLR9 inhibitory sequences | 7 |
| 3 | qPCR of human *SFTPB* gene expression shows increased expression with vectors containing TLR9i sequences | 7 |
| 4 | Survival curve shows TLR9i sequences permit readministration and improves median survival | 8 |
| 5 | Optimization of vector dosing | 31 |
| 6 | AAV vector assessment study to determine variability in efficacy | 40 |
| 7 | Human SFTPB levels by immunoblotting of ProSP-B and mature SP-B | 42 |
| 8 | Study timeline for gene expression analysis | 45 |
| 9 | Volcano plots show no gene expression changes after a single dose of AAV-hSPB with or without TLR9i sequences | 47 |
| 10 | Volcano plots show greatest gene expression changes with repeat dose of AAV-hSPB | 48 |
| 11 | Heatmap shows increased gene expression in interferon pathways after repeat dose of AAV-hSPB | 50 |
| 12 | Relative cell abundance of Th1 cells is greatest after a repeat dose of AAV-hSPB | 51 |
| 13 | *Mx1* and *Stat1* show significant differences between the no treatment (on dox) and AAV-hSPB repeat groups | 53 |
| 14 | Stat1 by immunoblotting validates qPCR and shows increased expression in AAV-hSPB repeat groups | 56 |
| 15 | Immunoblotting of Tbx21 confirms cell profiling of Th1 cells | 60 |

## List of Abbreviations

| | |
|---|---|
| **AAV** | Adeno-associated virus |
| **TLR9** | Toll-like receptor 9 |
| **TLR9i** | Toll-like receptor 9 pathway with inhibitory sequences |
| **SP-B** | Surfactant Protein-B |
| **Th1** | T-helper 1 |
| **ATII** | Alveolar type II |
| **SP-A** | Surfactant Protein-A |
| **SP-C** | Surfactant Protein-C |
| **SP-D** | Surfactant Protein-D |
| **IFN** | Interferon |

**Abstract**

SARAH ELYSSE ALLEN. Analysis of the Immune Response After Readministration of a Novel AAV6 Gene Therapy Containing TLR9 Inhibitory Sequences. (Under the direction of MARTIN KANG).

Therapeutic options for the treatment of Surfactant Protein-B (SP-B) deficiency, an autosomal recessive disorder that leads to fatal respiratory distress, are extremely limited with the exception of double lung transplantation. One method for treating this monogenic lung disease is with adeno-associated virus (AAV) gene therapy treatment that delivers the *hSFTPB* transgene into the lungs. The transient nature of AAV transgene expression led to a need for sustained gene expression, which could possibly be achieved through redosing. The main obstacle with redosing is the innate immune response and subsequent inflammatory response pathways that are activated after recognition of unmethylated CpG motifs in the AAV genome by toll-like receptor 9 (TLR9). Through readministration of an engineered AAV6.2FF vector with TLR9 inhibitory (TLR9i) sequences incorporated into the genome, prolonged survival in a mouse model of SP-B deficiency was demonstrated compared to a single dose of gene therapy. However, the specific gene or gene pathways impacted following TLR9 suppression have not been well characterized. I hypothesize that the incorporation of TLR9i sequences into the modified AAV6 vector genome will permit readministration through suppression of multiple immune response genes involved in the interferon pathways. This will be explored through two main aims: the production and purification of AAV vectors for assessment studies, and through exploration of gene expression analysis data to further characterize the

immune response after repeat doses of the gene therapy treatment with and without TLR9 inhibition.

To assess the immune response following TLR9 inhibition, RNA was isolated from lung tissue in mice treated with single or repeat doses of AAV with (AAV-hSPB$_{TLR9i}$) and without (AAV-hSPB) the TLR9i sequences, and analyzed by nCounter (Nanostring) gene expression analysis.

The gene expression analysis assessed over 700 different host response genes, with AAV-hSPB redosing treatment showing greater than 100 significant gene expression changes compared to less than 10 genes in mice redosed with AAV-hSPB$_{TLR9i}$. Several genes were further examined including *Serpina1a, Zbp1, Cxcl10, Stat1,* and *Mx1* due to their roles in regulating or responding to the immune response. Examination with qPCR, showed a significant increase in expression in genes involved in interferon response pathways including *Mx1* and *Stat1* following AAV-hSPB redosing but not AAV-hSPB$_{TLR9i}$ redosing. Another gene we examined was *Tbx21* (T-bet), a marker for T helper cells (Th1) by immune cell profiling, which showed the highest levels after a repeat dose of AAV-hSPB but was reduced with AAV-hSPB$_{TLR9i}$.

In conclusion, the AAV-hSPB$_{TLR9i}$ permits AAV redosing by suppressing multiple immune response genes including some involved in the interferon response pathway, as well as Th1 cells. For neonates with SP-B deficiency, the incorporation of the TLR9i sequences, and subsequent suppression of immune response genes, could allow for readministration of a gene therapy treatment to improve survival.

## 1.0 Introduction

### *1.1 Surfactant Protein-B*

Pulmonary surfactant forms a film across the alveolar surface, which reduces the surface tension and prevents lung collapse following exhalation. Surfactant is a mixture of lipids and proteins synthesized by alveolar type II cells (ATII). The ATII cells play a crucial role in maintaining pulmonary function and surfactant production to prevent atelectasis and subsequent respiratory distress[1]. Surfactant produced by the ATII cells reduces the surface tension at the air-liquid interface. Without surfactant the surface tension increases, and this leads to lung collapse in neonates[1]. Four of the surfactant proteins that make up pulmonary surfactant are Surfactant Protein-A (SP-A), Surfactant Protein-B (SP-B), Surfactant Protein-C (SP-C), and Surfactant Protein-D (SP-D) and they play an important role in surfactant structure and function[2].

### 1.2 Surfactant Protein-B deficiency

SP-B deficiency is a rare, autosomal recessive disease caused by mutations to both *SFTPB* gene copies leading to a lack of SP-B protein expression. This loss in protein expression results in abnormal pulmonary surfactant formation and subsequent impaired lung function that is fatal within the first few months of birth[1]. Exogenous pulmonary surfactant replacement therapy is ineffective in hereditary SP-B deficiency and the only current treatment option available is a double lung transplant. However, neonatal lung transplants come with a multitude of challenges such as size matching, donor availability, and unknown

risks associated with the long-term impact of immunosuppressive medications. Although there has been some success with neonatal lung transplants, most patients do not undergo the procedure[3]. This suggests that alternative therapies for SP-B deficiency are needed.

### *1.3 Use of adeno-associated virus (AAV) for a gene therapy treatment*

Adeno-associated virus (AAV) is a protein capsid containing a single-stranded DNA genome that is about 4.8 kilobases (kB) long[4]. Since its discovery in 1965, there have been many recent advancements with AAV for *in vivo* gene therapy treatment of hereditary diseases[5]. The US Food and Drug Administration (FDA) approved the first AAV gene therapy treatment for Leber's congenital amaurosis (Luxturna, AAV2) in 2017, then another AAV gene therapy treatment for spinal muscular atrophy (Zolgensma, AAV9) in 2019. In addition to those, the FDA recently approved another AAV gene therapy treatment for Hemophilia B, branded as Hemgenix in 2022, and Elevidys for Duchenne's muscular dystrophy in 2023. Unfortunately, the lungs have typically been classified as an inaccessible organ for viral vector-mediated gene therapy delivery due to the lack of effective vectors available to efficiently transduce the airway and the alveolar epithelium. Other barriers to delivering AAV gene therapy treatment to the lungs include the vector's ability to reach target cells and circumvention of the protective mechanisms enforced by the rapid immune response at recognition of foreign pathogens[6]. The efficacy of AAV vectors capable of transducing the lungs have been shown to be transient, along with therapeutic benefits waning over time. This may be partly due to ATII cell turnover[7]. A potential way to

overcome this latter problem is by incorporating toll-like receptor 9 (TLR9) pathway inhibitory oligonucleotide sequences into the vector genome as a way to evade the initial innate immune response against AAV DNA. Inhibition of the TLR9 pathway could allow for readministration of the vector, potentially overcoming the barrier of existing immunity to AAV6.

### *1.4 The role of the TLR9 pathway in the regulation of the innate and adaptive immune system*

Transducing the alveolar epithelium for the delivery of the AAV-mediated viral vectors poses a challenge due to the rapid immune response triggered by the recognition of the AAV. The AAV capsid coat and the transgene delivered by the AAV vector activate the innate and adaptive immune responses in the host which can impact transgene expression and prevents AAV re-administration[8]. There are many players involved in the initial response to AAV in the host immune system, but after exposure to unmethylated CpG motifs in the AAV genome, the TLR9-MyD88 pathway is primarily responsible for the activation and production of pro-inflammatory cytokines[9]. After exposure, the unmethylated CpG DNA motifs found in the AAV genome interacts with TLR9 receptor in the endosomes of dendritic cells, macrophages, B cells, T cells, epithelial cells and fibroblasts[9]. Following this binding of viral DNA to TLR9, the MyD88 adaptor protein is recruited, and this leads to downstream activation of NF-kB and type I interferon regulatory factors (Figure 1A). Subsequently, these downstream activations generate an innate immune response against AAV by the expression of proinflammatory cytokines, chemokines and various interferon genes[9]. This also

leads to downstream activation of the adaptive immune response that eventually targets and destroy the vector and AAV transduced cells[10]. These downstream effects hinder the ability to readminister AAV or dose patients that were previously exposed to AAV in the environment due to the humoral and cellular immunity activation following virus recognition[8].

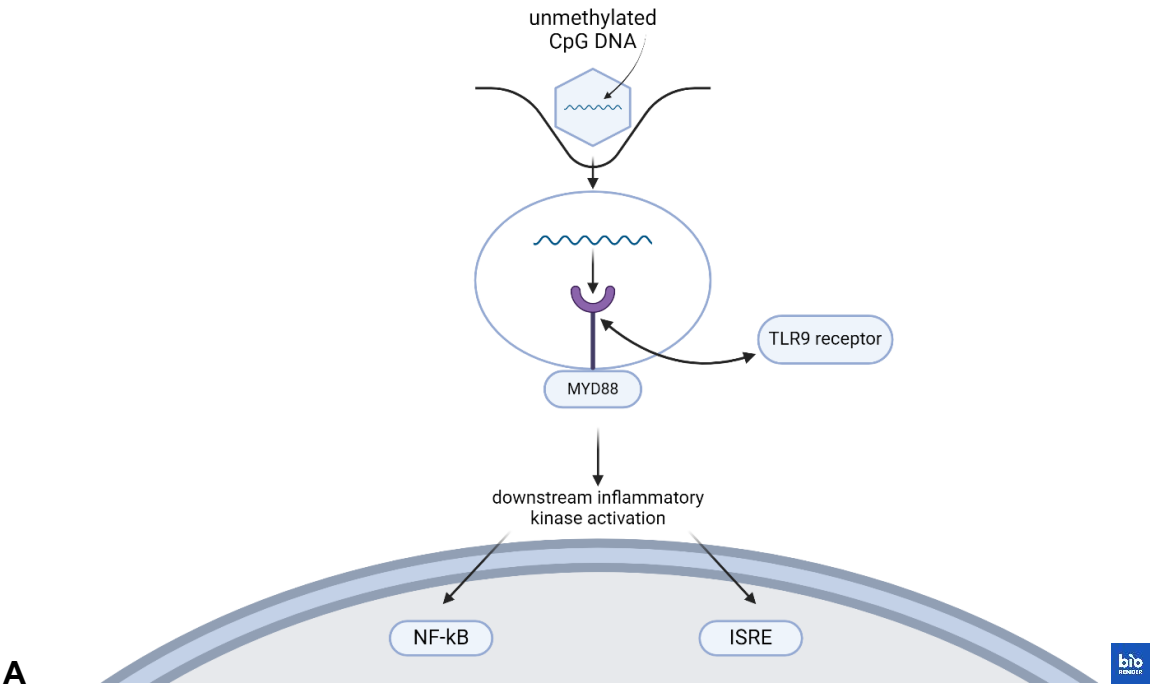


A

**Figure 1: Schematic of TLR9 pathway recognition of unmethylated CpG DNA motifs.**

(A) TLR9 pathway activation schematic demonstrating recognition of CpG DNA motifs activates TLR9-MyD88 relationship and subsequent inflammatory response cascades.

### *1.5 TLR9 Inhibition and its reduction in the inflammatory and immune response to AAV*

Activation of the TLR9 pathway promotes an increased immune response after exposure to AAV; consequently, the inhibition of this pathway could be a potential

method for reducing immunogenicity and enhancing the transgene expression in the lungs. Incorporation of the TLR9 inhibitory sequence (TLR9i) works due to the higher binding affinity that TLR9i has for TLR9 over the CpG DNA which prevents dimerization and innate immune activation[11]. The utility of TLR9i sequences incorporated into the AAV genome has been demonstrated to reduce the inflammatory and immune responses in vivo with multiple tissue types and administration routes[11]. These sequences were tested in mouse liver after an intravenous injection, skeletal muscle of mice after an intramuscular injection, mouse retina after an intravitreal injection, retina after a subretinal injection in outbred pigs, and retina after intravitreal injection in outbred macaques[11]. However, the effects of TLR9i on AAV efficacy in the lungs, or on AAV redosing were not explored.

### *1.6 Redosing of AAV using TLR9 inhibition*

The field of gene therapy has been rapidly advancing, and AAV is an attractive delivery method due to its relatively low immunogenicity. Even though it has been well established that AAV gene therapy can correct gene dysfunction, its efficacy does wane over time and is traditionally only offered as a single dose. One way to overcome this problem was to incorporate the TLR9i sequences into the AAV vector genome and evaluate the effects of readministration in the SP-B deficient mouse model[12]. By suppressing the innate and adaptive immune response to the AAV, the goal was to see whether redosing was possible through improved median survival rates among mice that received AAV-hSPB$_{TLR9i}$ [13]. The

AAV6.2FF vector used for these experiments contains the human *SFTPB* cDNA transgene (AAV-hSPB) (Figure 2A). TLR9 inhibitory sequences were incorporated into 5' to the CASI promoter and 3' to the polyA tail (AAV-hSPB$_{TLR9i}$) (Figure 2B). The CASI promoter consists of a human cytomegalovirus gene enhancer region, chicken beta actin promoter, and the human ubiquitin C promoter[7]. To evaluate these sequences, an inducible *Sftpb -/-* mouse, on a FVB/N background, that conditionally expressed SP-B under doxycycline supplementation was used[14]. After removal of doxycycline supplemented feed, the mice undergo respiratory distress and die within 4 to 11 days. A previous survival study in this mouse model has shown that vectors with the TLR9 inhibitory sequences lead to prolonged survival and improved body weight maintenance[15]. Results from qPCR show human *SFTPB* expression levels in mice that received gene therapy treatment, with no human *SFTPB* gene expression in the no treatment groups, as expected since only mice that received vectors containing the *hSFTPB* transgene would express this (Figure 4A). Median survival for mice that received repeat doses of AAV-hSPB$_{TLR9i}$ was 296 days. This surpassed the median survival for repeat doses of AAV-hSPB (122 days) (Figure 4A). Data indicated that positive signs of survival for this study included body weight, which was maintained closely in the repeat AAV-hSPB$_{TLR9i}$ group to the No Treatment (On Dox) group (Figure 4B-C)[7]. These results prompted the search for what genes or gene pathways were directly responsible for suppression of the TLR9 pathway, and evasion of the immune response.

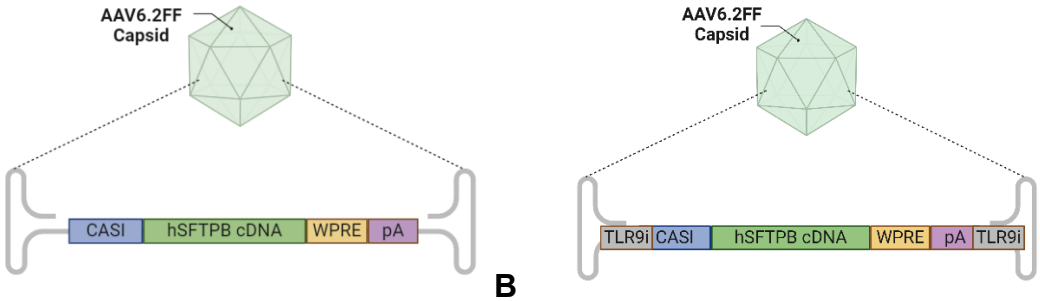


A B

**Figure 2: Contents of AAV6.2FF vector with and without TLR9 inhibitory sequences**

(A) Diagram of AAV6.2FF vector contents (B) Diagram of AAV6.2FF vector contents with 'io' (inhibitory oligonucleotides) placed 5' and 3' to the human *SFTPB* transgene

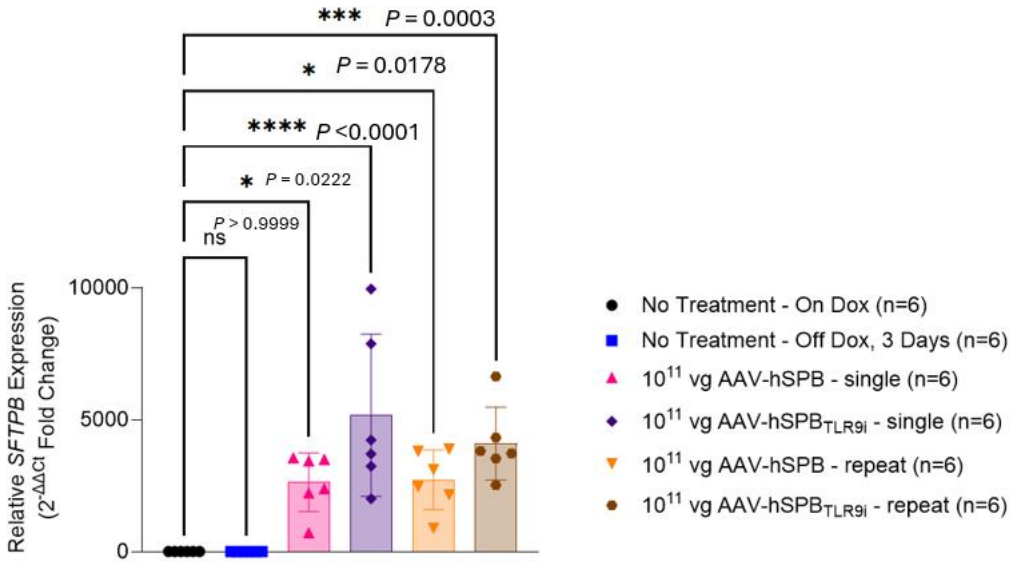


A

**Figure 3: qPCR of human *SFTPB* gene expression shows increased expression with vectors containing TLR9i sequences.**

(A) qPCR results of human *SFTPB* expression in mice at day 97 after AAV administration.

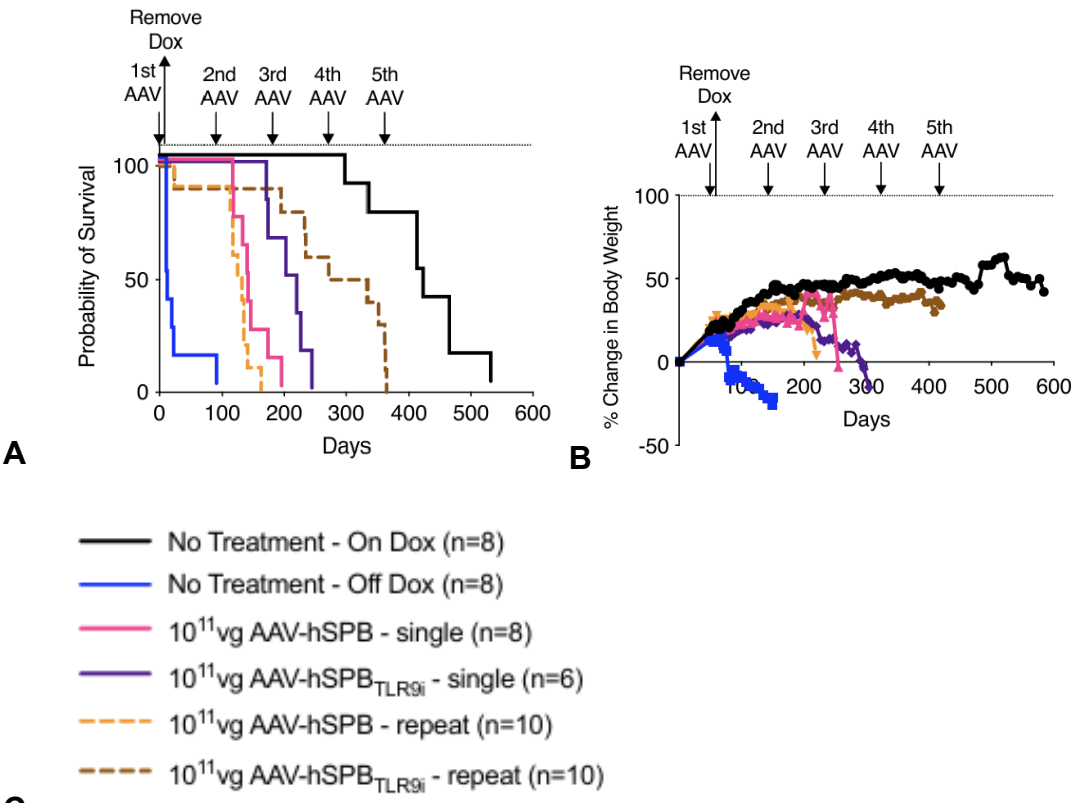


**Figure 4: Survival curve shows TLR9i sequences permit readministration and improve median survival**

(A) Kaplan-Meier survival curve from previously established data (B) % change in body weight of the mice as a method to assess overall health during the survival study. (C) Treatment groups that correspond to the survival curve and body weights figures.

## 2.0 Materials & Methods

### *2.1 Bacterial transformation of E. coli*

Bacterial transformation of *E. coli* was necessary to propagate plasmids for AAV vector production. Bacterial transformation was achieved by thawing a vial of One Shot Stbl3 chemically competent cells (Life Technologies, Carlsbad, CA) for each transformation on ice. There were four plasmids in total: puc19 (control), AAV-fLuc, AAV-fLuc$_{TLR9i}$, and pDGM6.2FF. AAV-fLuc contained the firefly luciferase reporter gene, while AAV-fLuc$_{TLR9i}$ had the same firefly luciferase transgene combined with TLR9i oligonucleotide sequences 5' and 3' to the reporter gene. The pDGM6.2FF plasmid has the Rep and Cap genes necessary for AAV packaging and capsid shell proteins. To each vial of cells, 100 ng/µL of plasmid DNA were added and gently mixed. The vials were incubated on ice for 30 minutes, followed by heat-shocking the cells for 45 seconds at 42°C without shaking. After removing the cells from the 42°C bath, the cells were recovered on ice for 2 minutes. Then, 250 µL of room temperature Super Optimal broth with Catabolite repression (S.O.C.) Medium (Life Technologies, Carlsbad, CA) was added to each vial. The vials were capped tightly and placed horizontally on a shaker (LabLine, USA) at 37°C for 1 hour at 225 rpm. After the incubation period, 25-100 µL from each transformation was spread on pre-warmed LB ampicillin plates and left to incubate overnight at 37°C, inverted. Colonies were selected the next day and analyzed by plasmid isolation, followed by gel electrophoresis.

### *2.2 Plasmid Purification*

#### *2.2.1 Mini prep*

The goal was to determine whether plasmid DNA was propagated by the bacteria. This was done with a GeneJET Plasmid MiniPrep Kit (Thermo Scientific, Vilnius, Lithuania). Bacterial culture (1 mL) was placed into a microcentrifuge tube, and centrifuged in the Eppendorf centrifuge 5425R (Hamburg, Germany) for 2 minutes at 8,000 rpm to pellet the bacteria. After centrifugation, the supernatant was discarded and the pelleted cells were resuspended in 250 µL of resuspension solution by either vortex or pipette. Then 250 µL of the Lysis Solution was added and mixed thoroughly by inverting (4-6 times) until the solution was viscous and slightly clear. Next, 350 µL of Neutralization Solution was added and mixed immediately by inverting 4-6 times. The tube was then centrifuged for 5 minutes at 12,500 rpm. After this, the supernatant was transferred to a GeneJET spin column and centrifuged for another 1 minute at 12,500 rpm. Any flow-through was discarded and the column was placed back into the same collection tube. Now, 500 µL of Wash Solution was added to the GeneJET Spin Column and centrifuged for 30-60 seconds, and the flow-through discarded. The tube was centrifuged for another 1 minute to remove any residual wash solution. Then, the GeneJET Spin Column was transferred into a fresh 1.5 mL microfuge tube and 50 µL of the Elution Buffer was added to the center of the column membrane in order to elute the plasmid DNA. This was left to incubate for 2 minutes at room temperature and then centrifuged for 2 minutes at 12,500 rpm. The column was discarded,

and the purified plasmid DNA was assessed by a NanoDrop spectrophotometer (NanoDrop Technologies, Wilmington, Deleware) to determine purity and then stored at -20°C.

### *2.2.2 DNA gel electrophoresis*

To validate that plasmid DNA was propagated and present in the bacterial colony, DNA gel electrophoresis was performed. For this experiment, we cast a 0.8 % agarose gel (125 mL 1X TBE and 1 g Agarose). Before cooling completely and while the gel was still not set, 10-12 µL of SYBR Safe DNA Gel Stain (Invitrogen, Carlsbad, CA) was added to visualize DNA. Then the agarose was poured into a cassette, and left to set for at least 30 minutes. Samples for the gel were made with 18 µL DNA and 2 µL of 10X loading buffer. The gel was placed in the chamber with the wells closest to the cathode. To the gel, 10 µL of ladder was added to the first well, and 10 µL of DNA sample in loading buffer added to the indicated wells. The gel was run on manual mode at 100V. Imaging of the gel was performed using the ChemiDoc Imaging System (Bio-Rad Laboratories, Hercules, CA).

### *2.2.3 Maxi prep for plasmid purification*

The plasmid purification process yielded the final product that was sent to the University of South Carolina Vector Core for AAV large-scale production. To isolate the bacteria, 50 mL conical tubes with cultures were centrifuged with the

Thermo Scientific Sorvall X Pro Series Centrifuge (Thermo Fisher Scientific) for 10 minutes at 4,000 x g. Then the supernatant was decanted, and the pellet left in the conical tubes. For purification, the Thermo Fisher PureLink HiPure Plasmid DNA Purification Kit (Invitrogen, Carlsbad, CA) was used. The HiPure Maxi Column was equilibrated with 30 mL Equilibration Buffer and allowed to drain by gravity flow. Then, 10 mL of Resuspension Buffer with RNase A was added to the cell pellets in the tubes. Then 10 mL of Precipitation Buffer was added and mixed immediately by inverting until homogenous. After, the lysed bacteria were centrifuged for 20 minutes at 4,000 x g at room temperature. The supernatant was then transferred to the equilibrated column and allowed to drain by gravity. Next, 60 mL of Wash Buffer was added to the column, and allowed to drain by gravity with all flow-through discarded. To elute, a sterile 50 mL conical tube was placed under the column, and 15 mL of Elution Buffer was added and allowed to drain by gravity. Then, 10.5 mL of isopropanol was added to the elute to precipitate DNA, mixed well and incubated at room temperature for 2 minutes. At this stage, the PureLink HiPure Precipitator kit (Invitrogen, Carlsbad, CA) was used. After attaching the precipitator to a 30 mL syringe, the DNA was loaded, placed over a waste container, and the plunger inserted. After pushing the plunger all the way down, the precipitator was unscrewed from the syringe, the plunger was pulled back out, and the precipitator re-attached to the syringe. Then 3 mL of 70% EtOH was added to the syringe to wash the DNA. The plunger was reinserted to push the ethanol through with the process of unscrewing the syringe and removing the plunger repeated. Once the syringe

was re-attached to the precipitator, the plunger was pushed back into the syring and then air was passed through the precipitator four more times. The precipitator was blotted with a Kimwipe and a new 5 mL syringe was attached, and 500 µL of TE Buffer was added and pushed through. After removing the syringe and re-attaching, the same TE buffer was placed on the column and reeluted. This final product was collected in a microfuge tube and analyzed for DNA concentration and purity by a NanoDrop spectrophotometer. DNA purity was measured in ratios of A260/A280 and A260/A230.

### *2.2.4 AAV Production and Purification*

Human Embryonic Kidney (HEK) 293 cells were thawed and added to a tube with PBS and spun to pellet. The PBS was discarded to remove residual dimethylsulfoxide (DMSO). Dulbecco's Modified Eagle Medium (DMEM) was added and then cells were transferred to 15 cm dishes. Cells were split until the desired amount was achieved for transfection. The following day the cells were split 1:2 for transfection, aiming for 85-90% confluency. Transfection master mix was prepared for DNA mixture, and once the DNA precipitate was generated, this was added to dishes and allowed to incubate. Cells and viruses were harvested 3-5 days after transfection. After harvesting the cells, they were placed in media mixture and autoclaved. The contents were centrifuged and the supernatant decanted and saved. Then, lysis buffer was added to the pellet and resuspended. The cells were left to incubate in the lysis buffer for one hour at 37°C. The contents were centrifuged once more, and the supernatant was

decanted into the same container containing supernatant from the previous step. This crude vector lysate was then purified by density gradient centrifugation by the University of South Carolina Viral Vector Core and titers calculated by qPCR of inverted terminal repeat sequences in the AAV genome.

### *2.3 Animal Model*

The preclinical animal model used for this research was an inducible, mouse model of SP-B deficiency on an FVB/N background under the control of a doxycycline-dependent promoter[14]. SP-B -/- mice die immediately after birth, so these triple transgenic mice were generated to allow for assessment of SP-B deficiency in lung function after birth.[14] These compound transgenic mice were generated to conditionally express SP-B under the control of reverse tetracycline transactivator (rtTA) protein in the ATII cells, and thereby produce SP-B in response to intake of doxycycline supplemented feed. These mice were maintained on a doxycycline-supplemented diet (0.625 g/kg doxycycline hyclate: Teklad) and were caged in an individually ventilated cage system with no more than five animals housed per cage. The mice were identified by an assigned numerical identification number, and ear-notched. Removal of the doxycycline-supplemental diet induces surfactant deficiency and signs for respiratory distress can be observed to track disease progression for survival studies.

All animal procedures are approved by the Medical University of South Carolina Institutional Animal Care and Use Committee (IACUC-2022-01404) and are in compliance with the university guidelines, state, and federal regulations.

### *2.4 AAV Administration*

#### *2.4.1 Anesthesia by intraperitoneal injection of Ketamine/Xylazine*

A mixture of ketamine and xylazine, anesthetic and analgesic respectively, was used to keep the mice under a plane of anesthesia for the intubation and AAV administration procedure. The working dose of ketamine was 100 mg/mL and 10 mg/mL for xylazine. Mice were dosed by weight. The two mice in the study were dosed at a ratio of 80/8 ketamine/xylazine at the working doses by an intraperitoneal injection and placed back into their cage on a warming pad until sufficiently anesthetized. Anesthesia was confirmed by non-responsiveness to a toe-pinch.

#### *2.4.2 Subcutaneous injection of saline*

Once it was confirmed that the mouse was anesthetized, 1 cc of normal saline was injected subcutaneously on the dorsal side to provide hydration during the procedure. Additionally, using a 1 mL syringe without a needle, a drop of saline was placed on each eye to keep the eyes moistened to prevent post-procedure irritation.

### *2.4.3 Intubation and Endotracheal delivery of AAV*

The delivery method for this experiment was by intubating the mice and delivering the AAV through an endotracheal tube. Each mouse was placed on an intubation stand with a loop of surgical thread to allow mice to hang supine at just under 90 degrees by their incisors. A beam of light was placed on the tracheal surface of the mouse to allow for visualization of the airway. After moving the mouse tongue to the side, the tracheal opening was seen with proper light placement. The guide device was inserted into the mouth and towards the tracheal opening. To confirm that the tube entered the trachea and not the esophagus, a 1 mL syringe with water was attached to the endotracheal tube. If oscillation was observed, the tube was successfully in the trachea. Then, the 1 mL syringe with water was removed from the endotracheal tube, and a 1 mL syringe with the AAV dose was placed in the tube and the plunger pushed down. This was followed by three separate administrations of air to improve vector delivery through the lungs. The mouse was left in this upright position to recover for at least 1 minute. Once regular breathing returned, the mouse was removed from the intubation stand and placed into its cage on a heating pad to recover and monitored for a short period of time. After the breathing returned to a regular rhythm, each cage was returned back to the rack. Post-procedure checks were done 2-3 hours after administration, and the day after intubation. At 3 days post administration, all mice that received AAV were changed into fresh cages. Following this procedure, these mice were used for vector potency and vector assessment studies to assess the vectors from the USC Viral Vector Core.

### *2.5 RNA Extraction for gene expression analysis*

For gene expression analysis, lung tissue was isolated by excising the right lung from the chest cavity of mice, and were then placed in cryogenic vials and snap-frozen with liquid nitrogen. RNA was extracted from murine lung tissue for gene expression analysis of the host immune and inflammatory response after AAV administration. In 15 mL tubes on ice, 600 µL of lysis buffer (5 mL lysis buffer + 50 µL of 2-mercaptoethanol) was added to each tube. The ratio of lysis buffer to lung tissue was 600 µL lysis buffer for every 30 mg of lung tissue. The lung tissue was mechanically homogenized for 30-40 seconds at 25,000 x g (maximum speed) three times. To prevent cross-contamination, the rotor was washed and cleaned with 70% ethanol and RNase Zap between sample homogenizations. The homogenized sample was then transferred to a 1.5 mL microfuge tube. The microfuge tubes were centrifuged for 5 minutes at 2,600 x g at room temperature (20-22°C). After centrifugation, the supernatant was transferred to a 15 mL conical tube. To the tubes, 1 volume of 70% ethanol was added to the homogenate to match the volume of supernatant, and then vortexed. Carefully, 700 µL was transferred at a time to a spin cartridge and centrifuged for 15 seconds at 12,000 x g. The flow-through was discarded, and the spin cartridge re-inserted to the same collection tube, this was repeated until

finished. Next, wash buffers were added to the spin cartridge and centrifuged for 15 seconds at 12,000 x g at room temperature, and the flowthroughs discarded. Following washing, the spin cartridge was then centrifuged for 1 minute at 12,000 x g at room temperature to ensure the membrane containing bound RNA was dried. The spin cartridge was then inserted into a recovery tube and 30 µL of RNase-free water was added to the spin cartridge to elute RNA. This was incubated at room temperature for 1 minute and then centrifuged for 2 minutes at ≧ 12,000 x g at room temperature, and then the spin cartridge was discarded. Finally, the RNA concentration and purity were assessed by a Nanodrop spectrophotometer.

### *2.6 Gene expression analysis*

Following RNA extraction from lung tissue, 100 ng of RNA was hybridized to the Mouse Host Response Panel CodeSet overnight (nCounter Pro MAX/Flex, Nanostring). The nCounter Prep Station automatically processed the samples, and then the cartridge containing the probes bound to immobilized RNA were scanned at 555 fields of view for image acquisition. The barcodes were counted and analyzed through the nCounter software (nSolver 4.0). The raw RCC files were used to analyze quality control (QC) issues by nSolver and no QC files were flagged from any samples. With ROSALIND, the raw RCC files were imported into the system and used to generate volcano plots and bar graphs of the normalized gene expression changes and cell profiling results.

### *2.7 qPCR validation of genes from gene expression analysis*

Results from the gene expression analysis by nCounter yielded volcano plots that showed genes with significant changes between treatment groups. Genes were chosen to be validated based off of their role in the interferon response pathway which is affected by the TLR9 pathway, and other genes chosen due to their key part in the innate immune response to foreign pathogens. To validate these genes by qPCR, we first generated cDNA by combining RNA (µL) in a master mix made of: 10X RT buffer, 25X dNTP mix, 20% 10X RT random primer, 10% reverse transcriptase, and water. For qPCR analysis, 2µL of cDNA plus 18 µL of a component mixture (Mastermix, Gene & Nuclease-free water) were added to each well on a 96-well plate and run on the Quant Studio 3 real time PCR machine. The results were exported to .xls files and analyzed by Excel. All genes were compared to the reference gene, GAPDH, to generate bar graphs of relative expression for each gene.

### *2.8 Protein isolation of murine lung tissue for validation experiments*

Protein was isolated from snap-frozen harvested murine lung tissue. A Roche protease inhibitor tablet was added to 50 mL of TX-100 lysis buffer, and chilled on ice. A total of 100 mg of frozen lung tissue was added to 2 mL lysis buffer in a 15 mL conical tube for all lung samples. In the case of smaller lung harvests, only 50 mg of tissue was collected and added to 1 mL of TX-100 lysis buffer. The

contents of each tube were mechanically homogenized for 1 minute each at maximum speed. Samples were placed back on ice after each round of homogenization, until each had been homogenized 3 times. The rotor was washed and cleaned between each sample with 70% ethanol and $dH_2O$, and then the samples were each transferred to 2 mL tubes and centrifuged at 20,000 x g for 15 minutes at 15ºC to remove insoluble cell debris. After centrifugation, the supernatant was collected into three separate 1.5 mL tubes at equal volumes and stored at -80ºC.

### *2.9 Bradford assay of murine lung homogenate*

The lung tissue lysates were analyzed in a Bradford Assay to measure protein concentration for Western blotting. To run this assay, 2.5 µL of each tissue lysate sample was added to 250 µL of Coomassie Brilliant Blue in a 96-well plate. This plate was analyzed using the BioGen plate reader at 600 nm, and the resulting absorbance values were transferred to Excel software. In Excel, each value was normalized to the blank and then graphed on a line with a best-fit trendline to generate an $R^2$ value and line equation. The line equation was generated from standards that were made with the Pierce™ Bovine Serum Albumin Standard Ampules (Thermo Fisher, Carlsbad, CA). The formula was used to determine the protein concentration of each sample, and could identify the volume to load into the wells of a SDS-PAGE gel so that each well contained 20 µg of protein.

### *2.10 Western blotting*

Western blotting was performed to validate human *SFTPB* expression as well as key immune and inflammatory response genes of interest. After it was determined how much volume of each sample to load by the Bradford Assay, samples were prepared in microfuge tubes with equal volumes of sample and 2X Laemmli buffer, the loading buffer. Once combined and mixed by pipetting, the samples were heated to boiling at 100ºC for 10 minutes. Samples were either loaded onto a 10% BioRad precast Mini-Protean gel immediately, or stored at -20ºC overnight and used the next day. The running buffer was 1X Tris-Glycine buffer. After the gel and cassette were assembled into the BioRad Mini-Protean Vertical Electrophoresis Cell (Bio-Rad, USA), the wells were washed out twice with running buffer and then the samples loaded. The gel was run at 70 V until the dye front reached the bottom of the gel and then the gel was removed from the cassette. Once the plastic plates were removed, the wells and bottom edge of the polyacrylamide gel were trimmed and transferred into deionized (DI) water to clean off any excess polyacrylamide. After cleaning, the gel was transferred to 1X Transfer Buffer, made of 25X Transfer Buffer + 10% methanol + DI water, to incubate for 25 minutes on the rocker at room temperature. The filter papers used for transfer were soaked in 1X Transfer Buffer for 8 minutes, and the 0.45 µm PVDF membrane was activated in methanol for 10-15 seconds prior to incubating in 1X Transfer Buffer for 2-3 minutes. For transfer, the BioRad Trans-Blot SD Semi-Dry Transfer Cell apparatus (Bio-Rad, USA) was used. First the anode electrode was wet completely with transfer buffer, then the filter paper

added, then PVDF membrane, any air bubbles were rolled out, the gel was then carefully placed on the membrane with the air bubbles rolled out once again, and then the sandwich was completed with the final filter paper on top and a final roll to remove any air bubbles. The top cathode electrode of the transfer apparatus was wet with transfer buffer as well, then placed on top of the membrane and gel. The transfer step was run at 15V for 15 minutes. Once transfer was complete, the membrane was placed immediately into 5% blocking buffer (2.5 g non-fat milk powder + 50 mL PBS-Tween-20) for 1 hour at room temperature on a rocking platform. After the blocking step was over, the blot was washed 3 times for 5 minutes each with PBS-T. The final wash was when the blot was cut, and then placed into two different trays to incubate in their respective primary antibodies (see below).

Primary antibody incubation was always performed overnight at 4ºC on a rocking platform. Each blot was washed 3 times for 5 minutes with PBS-T. Secondary antibodies were then added to each blot and incubated at room temperature on the rocker for one hour. After secondary incubation the blot was washed again three times for five minutes each with PBS-T. In order to visualize the protein bands, ECL SuperSignal West Pico Plus (Thermo Fisher, Carlsbad, CA) or Pierce ECL Substrate (Thermo Fisher, Carlsbad, CA) was used. Incubation for ECL SuperSignal West Pico Plus was 5 minutes, and Pierce ECL Substrate was 1 minute. After incubation, the ECL was removed, and the blot placed in water. Imaging of the blot was by the ChemiDoc Imaging System with varying exposure settings on chemiluminescence. The PageRuler Prestained Protein Ladder

(Thermo Fisher, Vilnius, Lithuania) was visualized on the auto-rapid colorimetric setting to estimate the size of the protein bands.

### *2.10.1 ProSP-B*

Western blotting of proSP-B was used to confirm expression of human SP-B protein, as this was what was delivered to each mouse by the AAV6.2FF vector. The primary antibody used for SP-B visualization was from Santa Cruz Biotechnology (sc-133143) at 1:100 dilution, with goat α-mouse IgG H+L secondary antibody, HRP (Thermo Fisher Scientific, Rockford IL), at a 1:5000 dilution. This antibody recognizes proSP-B which has an approximate size of between 45-50 kDa.

### *2.10.2 Mature SP-B*

Visualization of the isoforms of mature form of SP-B migrate as several bands migrating from about 8-44 kDa, with primary forms at 26 and 42 kDa. The primary antibody used for this was anti-SP-B (rabbit antiserum) (Millipore, USA). The secondary antibody was goat α-rabbit IgG H+L, HRP (Invitrogen, Rockford, IL) at a dilution of 1:1000.

### *2.10.3 Tbx21*

Visualization of the Tbx21 protein by western blotting was done to identify changes in Th1 cell levels between treatment groups. The primary antibody used for Tbx21 was anti-Hu/Mo T-bet (Invitrogen, Carlsbad, CA) at 1:250 dilution, with goat α-mouse IgG H+L secondary antibody, HRP (Thermo Fisher Scientific, Rockford IL), at a 1:5000 dilution. This antibody identifies a Tbx21 migrating at approximately 58 kDa.

### *2.10.4 Stat1*

Visualization of the Stat1 protein by western blotting was done to validate qPCR results of increased *Stat1* expression in the repeat AAV-hSPB group compared to the no-treatment on dox group. This protein is estimated to be 87 kDa, with two isoforms at: 84 kDa and 94 kDa. The primary antibody used for this was a Stat1 monoclonal antibody Stat1-79 (Thermo Fisher, CAT# AHO0832). The dilution was 1:500 for the primary antibody. The secondary antibody for this blot was goat α-mouse IgG H+L secondary antibody, HRP (Thermo Fisher Scientific, Rockford IL), at a 1:5000 dilution.

### *2.10.5 GAPDH*

GAPDH was used as a reference protein for some western blots, and this protein has an approximate molecular mass of 36 kDa. The primary antibody used for immunoblotting was α-GAPDH mAb (Invitrogen, Vilnius, Lithuania). The

secondary antibody was goat α-mouse IgG H+L secondary antibody, HRP (Thermo Fisher Scientific, Rockford, IL) at a 1:5000 dilution.

### *2.10.6 Vinculin*

Vinculin was also used as a reference gene for some western blots, and migrates at relative molecular mass range of 117-120 kDa. The primary antibody used was Vinculin mAb (ProteinTech, Rosemont, IL) at a 1:5000 dilution. The secondary antibody used was goat α-mouse IgG H+L secondary antibody, HRP (Thermo Fisher Scientific, Rockford, IL) at a 1:5000 dilution.

### *2.10.7 Histone H3*

Histone H3 was also used as a reference gene for some western blots, and its primary isoform migrates at a relative molecular mass of 15-17 kDa. The primary antibody used was Histone H3 mAb (Cell Signaling Technology, Danvers, MA) at a 1:1000 dilution. The secondary used was goat α-mouse IgG H+L secondary antibody, HRP (Thermo Fisher Scientific, Rockford, IL) at a 1:5000 dilution.

## *2.11 Serum collection by saphenous vein bleeds*

Serial serum collection was by saphenous vein bleeds. After placing each mouse in plastic restrainers, the leg was shaved, and coated with Vaseline to

enhance visualization of the saphenous vein. A 26-gauge needle was used to draw blood from the saphenous vein, and a capillary tube (Microvette®, Nümbrecht, Germany) collected the blood. We were careful not to collect more than 200 µL of blood., The tube was capped at the end and top, then placed in a vial at room temperature for a minimum of 10 minutes. To staunch blood flow, gauze pads were held at the needle puncture until clotting was achieved. If the mouse was still bleeding, the gauze pads were held at the wound site for an additional 1 minute. Once blood flow was successfully staunched, the mouse was placed back in its cage. To isolate serum from the blood, the tubes were centrifuged at 8,000 x g for 10 minutes at 4°C, after sitting at room temperature for at least 10 minutes. The serum was observed as clear or light-yellow above the blood cells, and were aspirated by a pipette and placed into a labeled Eppendorf tube and stored at -20°C.

### *2.12 Serum antibody levels by ELISA*

Enzyme-linked immunosorbent assay (ELISA) were used to quantify antibody levels to AAV6 and AAV6.2FF. This assay was done in a two-day process. The first day required coating a 96 half-well high affinity plate with a coating solution containing the AAV capsid coat of interest. For AAV6, a final titer of 1 x $10^{10}$ transducing units (TU)/mL was made from an original stock concentration of 1.06 x $10^{15}$. To achieve this, an intermediate stock (5 x $10^{12}$ TU/mL) was placed into 3 mL PBS and mixed. For AAV6.2FF, a concentration of 1 x $10^{10}$ vg/mL, was mixed

into 3 mL PBS. To each well, 30 µL of the diluted AAV was added to the plates in a tissue culture hood, and the plates were sealed and stored at 4°C overnight.

On day two, the serum samples were thawed on ice. The AAV coating solution from the plate was decanted, and the wells were washed three times with PBS 0.2% Tween-20, and then 30 µL of SuperBlock™ blocking buffer in PBS (Rockford, IL) was added to each well. Then, sample dilutions were made. For these ELISA assays, dilutions of serum in blocking buffer were made at 1:400, 1:800, 1:1600, 1:3200, 1:6400, 1:12800, 1:25600, 1:51200. The positive control was an anti-AAV6 mouse monoclonal antibody (ADK6) (Progen, Wayne, PA) made to 1:400, and 30 µL of the diluted positive control was added into the last two wells of the plate. For the blanks, wells received 30 µL of just blocking buffer. For all other dilutions, 30 µL of each was added in duplicate for each sample. Then the plate was sealed and incubated at 37°C for 1 hour. After, the dilutions were decanted, and the wells washed three times with PBS 0.2% Tween-20. Then, secondary antibody solution (3 mL blocking buffer and 1:1000 goat α-mouse) was made, and 30 µL added to each well. The plate was sealed once more, and incubated at 37°C for one hour. Finally, the secondary antibody was decanted, and the wells washed three times with PBS 0.2% Tween-20, and 30 µL of TMB solution (2 mL of each bottle) was added to the wells and incubated on a rocker at room temperature for 15 minutes. After incubation, any air bubbles were removed with a needle, and the plate was read at 600 nm on the BioTek Syngergy HT (Winooski, Vermont) machine with the Gen 5 1.11 software. A positive reciprocal titer from an ELISA assay was established as a color change

at 600 nm that was two-fold greater than the mean of ten negative control wells on the same plate[16].

### *2.13 AMI HT imaging*

The AMI HT imaging system was used to observe the mCherry and firefly luciferase reporter genes at multiple timepoints before and after AAV administration. Imaging of firefly luciferase required preparation within 24 hours of D-Luciferin substrate at a concentration of 15 mg per mL in 1xPBS. Mice were anesthetized with isoflurane, and 150 mg per kg of D-Luciferin was injected into each mouse 15 to 30 minutes before imaging. Mice were then anesthetized with isoflurane until even breathing with minimal movements. Then, the mice were placed with the ventral side facing the camera. The parameters for mCherry imaging were selected as 570 nm for excitation and 630 nm for emission. Parameters for firefly luciferase were set under the bioluminescence setting. Images were captured at 5% excitation power. After imaging, the mice were placed back in their cages. Files (.ami format) were downloaded from the computer onto an external USB drive for quantification in Aura.

### *2.14 ROI quantification*

Region of interest (ROI) quantification from the in vivo imaging using the AMI HT was performed on whole body and lung region of the mice to quantify mCherry expression. The software used was Aura, Spectral Instruments Imaging. The

files were uploaded, and ROIs were manually drawn over the lung, and over the whole body. The software generated measurement data for total emission (photons/s) and Maximum Radiance (photons/s/cm$^2$/steradian).

### *2.15 Western blot quantification*

Western blots were quantified with ImageJ software. Files from the ChemiDoc Imaging System (.TIFF format) were uploaded into ImageJ for analysis.

### *2.16 Statistical analysis*

Statistical analysis was performed with GraphPad Prism 10 software.

## *3.0 Results*

### *3.1 Vector production and generation*

AAV vectors were generated at the University of South Carolina (USC) Viral Vector Core Facility. Plasmids containing the capsid coat (AAV6.2FF) and transgenes (hSPB, hSPB$_{TLR9i}$, fLuc, fLuc$_{TLR9i}$) were shipped to USC, and vectors (AAV6.2FF-hSPB, AAV6.2FF-hSPB$_{TLR9i}$, AAV6.2FF-fLuc, and AAV6.2FF-fLuc$_{TLR9i}$) were returned at titers ranging from $10^{13}$ transducing units (TU)/mL to $10^{15}$ TU/mL. We also received AAV2- and AAV6-mCherry from the USC Vector core. With these vectors we began experiments to determine AAV vector potency and if pre-existing immunity to AAV6 could be overcome with vectors containing

TLR9 inhibitory sequences (AAV-hSPB$_{TLR9i}$) in comparison to the original vector, AAV-hSPB. This was achieved by conducting a survival study alongside serial serum antibody assessments and in vivo imaging after exposure to AAV6-mCherry (Figure 5A). However, after performing serial serum collections before and after initial “environmental” (AAV6-mCherry) exposure, we noticed that the mice had no mCherry signal from the in vivo images and ROI quantification, and did not have anti-AAV6 antibody levels in line with previously measured levels following a dose of $10^{11}$ vector genomes/mouse of AAV (Figure 5B-D)[16]. These initial results suggest the potency of the AAV vectors from the USC vector core did not achieve similar levels as other AAV preparations. These same two mice were then administered a higher dose of $10^{12}$ TU/mouse of AAV-hSPB and AAV-hSPB$_{TLR9i}$ and a survival study was performed. The survival curve between the two mice shows that the mouse that received AAV-hSPB$_{TLR9i}$ died at 23 days and AAV-hSPB died at 49 days after removal of doxycycline (Figure 5E). Removal of doxycycline terminates SP-B expression, and the mice typically die within 4-11 days without intervention. Survival to 23 days indicates the vector prolonged survival, but not as long as expected. Body weights of the mice show the rapid decline of weight associated with surfactant deficiency as the vector efficiency waned (Figure 5F). This suggests the AAV vectors from USC do work but not as effectively as vectors from other vector production facilities. As a result, we began a new experiment to test higher vector doses of vectors from the USC Viral Vector Core.

A

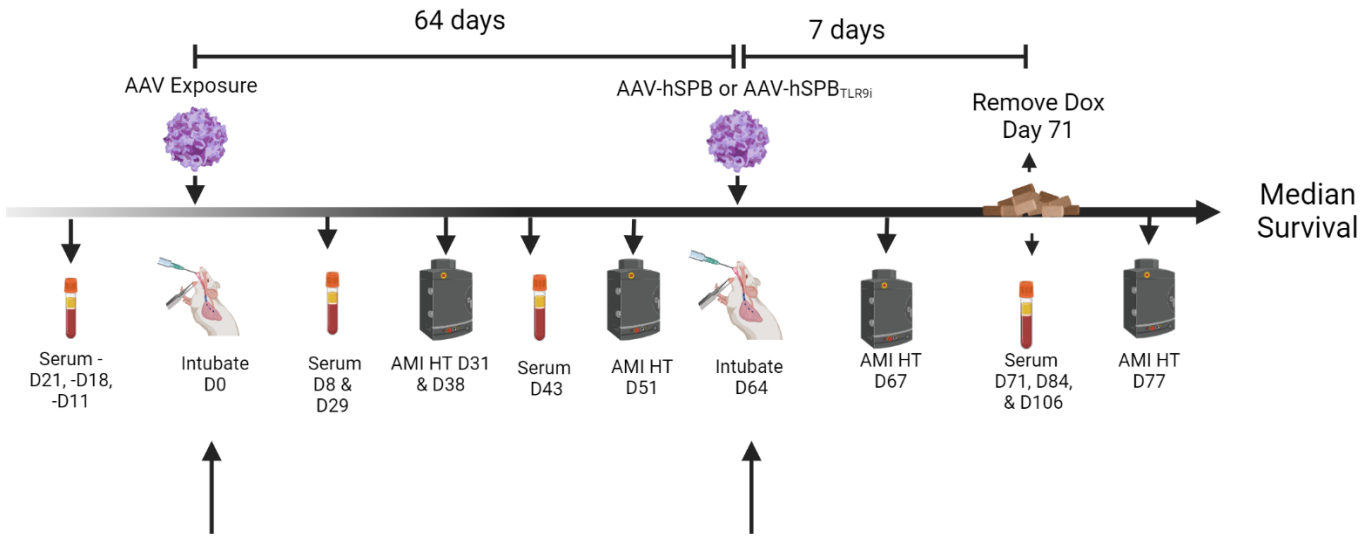


**AAV "Environmental" Exposure:**

All mice received $10^{11}$ vg/mouse AAV6-mCherry

**AAV Treatment:**

1. $10^{12}$ vg/mouse AAV6.2FF-hSPB (n=1)
2. $10^{12}$ vg/mouse AAV6.2FF-hSPB$_{TLR9i}$ (n=1)

**B**

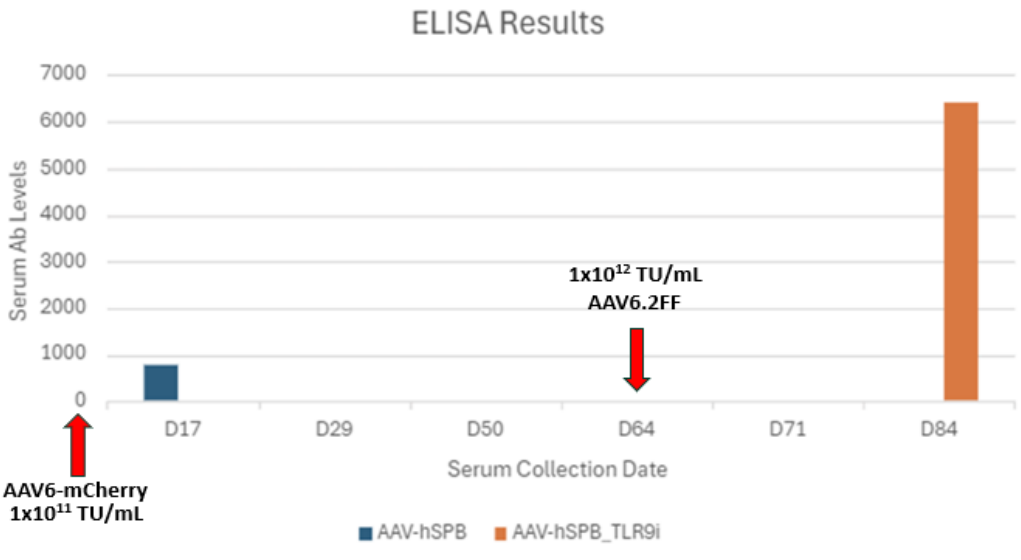
ELISA Results
7000
6000
5000
4000
3000
2000
1000
0
Serum Ab Levels
1x10^12 TU/mL
AAV6.2FF
AAV6-mCherry
1x10^11 TU/mL
D17
D29
D50
D64
D71
D84
Serum Collection Date
AAV-hSPB
AAV-hSPB_TLR9i

C

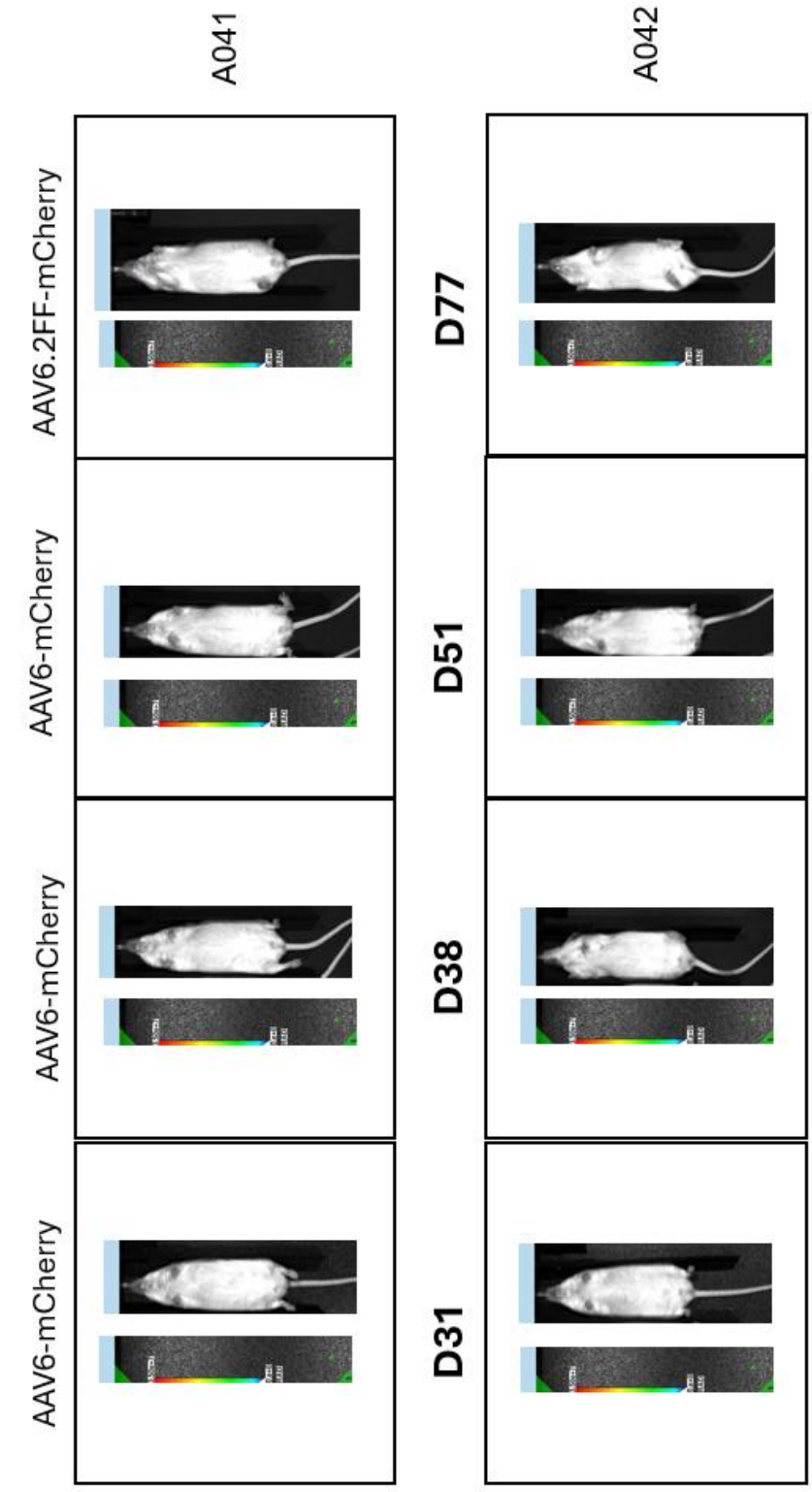
AAV6-mCherry
AAV6-mCherry
AAV6-mCherry
AAV6.2FF-mCherry
A041
A042
D31
D38
D51
D77

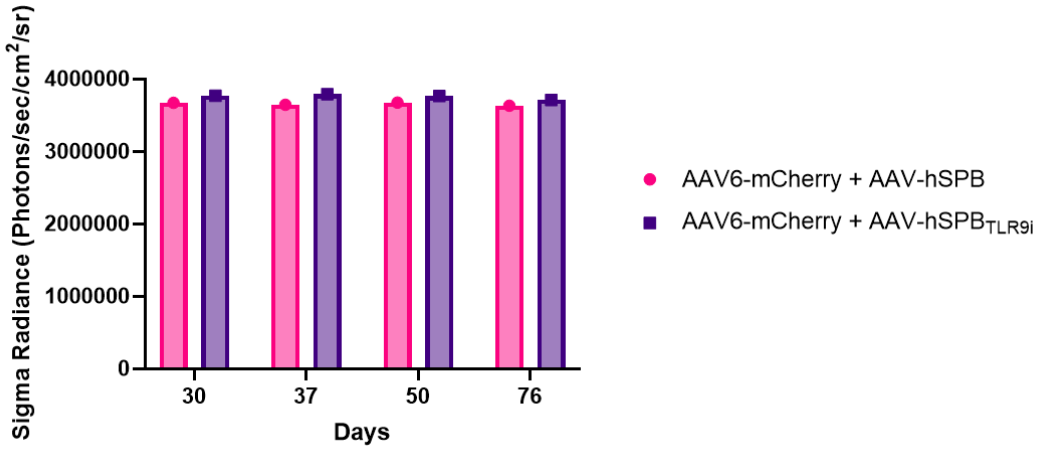
Sigma Radiance (Photons/sec/cm²/sr)
4000000
3000000
2000000
1000000
0
30
37
50
76
Days
AAV6-mCherry + AAV-hSPB
AAV6-mCherry + AAV-hSPBTLR9i

**D**

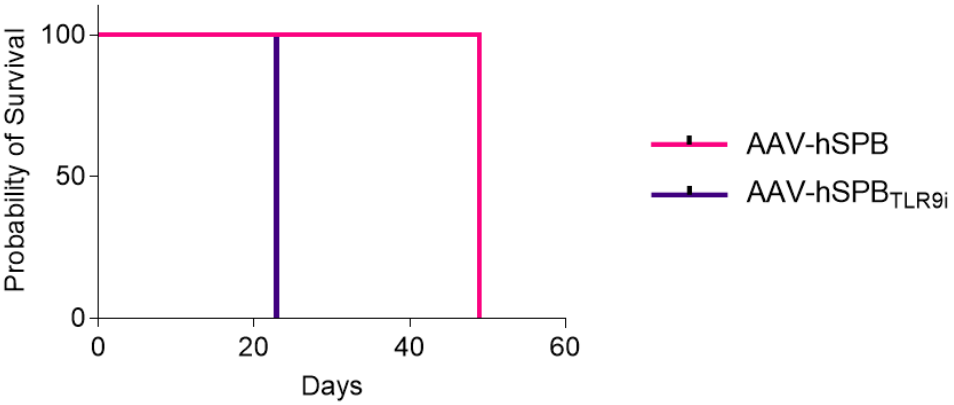
Probability of Survival
100
50
0
0
20
40
60
Days
AAV-hSPB
AAV-hSPBTLR9i

**E**

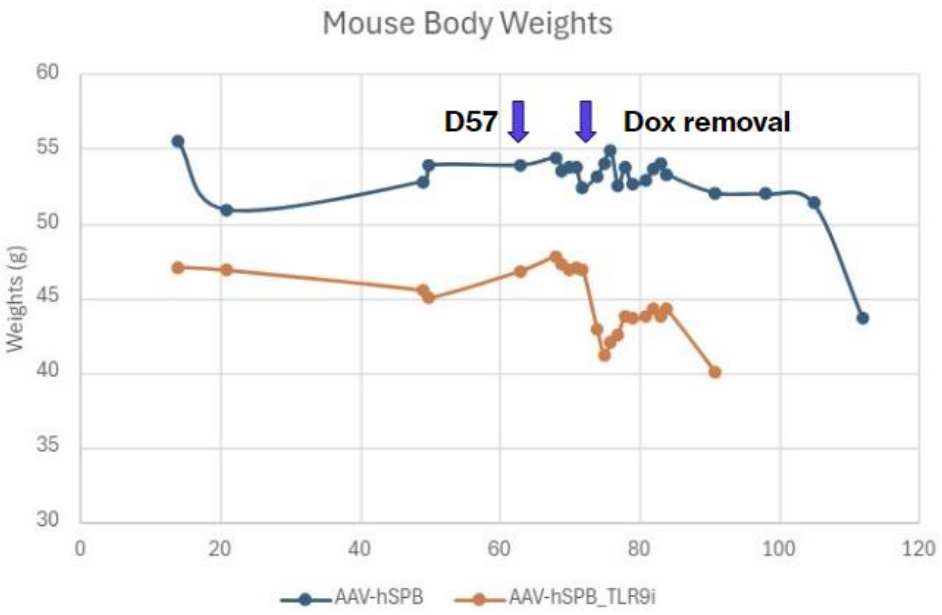


F

**Figure 5: Optimization of vector dosing**

(A) Study design to assess AAV vector potency and assess preexisting immunity (B) Serum Ab levels by ELISA assay results (C) AMI-HT images showing no fluorescence signal following AAV6-mCherry dosing (D) Quantification of mCherry levels showing no difference in expression between the 2 mice (E) Kaplan Meier survival curve. (F) Body weights over time of AAV-hSPB and AAV-hSPB$_{TLR9i}$ treated mice on and off doxycycline.

### *3.2 Vector assessment study*

To further assess the efficacy of the vector, an assessment study was done to establish which vectors performed optimally by comparing groups (AAV2-mCherry (USC), AAV6-mCherry (USC), AAV6.2FF-mCherry (Guelph/OHRI) and AAV6.2FF-fLuciferaseTLR9i (Guelph/OHRI)) through serial serum antibody measurements and in vivo imaging (Figure 6A). In vivo imaging of mice at Day 7

and Day 21 after AAV administration shows no fluorescence signal in any group, but there was bioluminescent signal in the right lung of one mouse in the AAV6.2FF-fLuciferaseTLR9i group with the vector from Guelph/OHRI that had been used in a previous study and shown to work (Figure 6B). The mCherry levels were quantified and showed negligible fluorescence signal for all groups (Figure 6C). The firefly luciferase expression was also quantified and did show the highest luciferase expression at Day 7 after AAV administration with waning expression into Day 21 (Figure 6D). Since the AMI-HT in vivo imager was not as sensitive to fluorescence, the thorax region was shaved to improve sensitivity, but as seen from Day 21 (Figure 6B) this still did not show any signal. The mice were imaged with a different apparatus, the MAESTRO imager, and there was no mCherry signal visualized (Figure 6E).

A

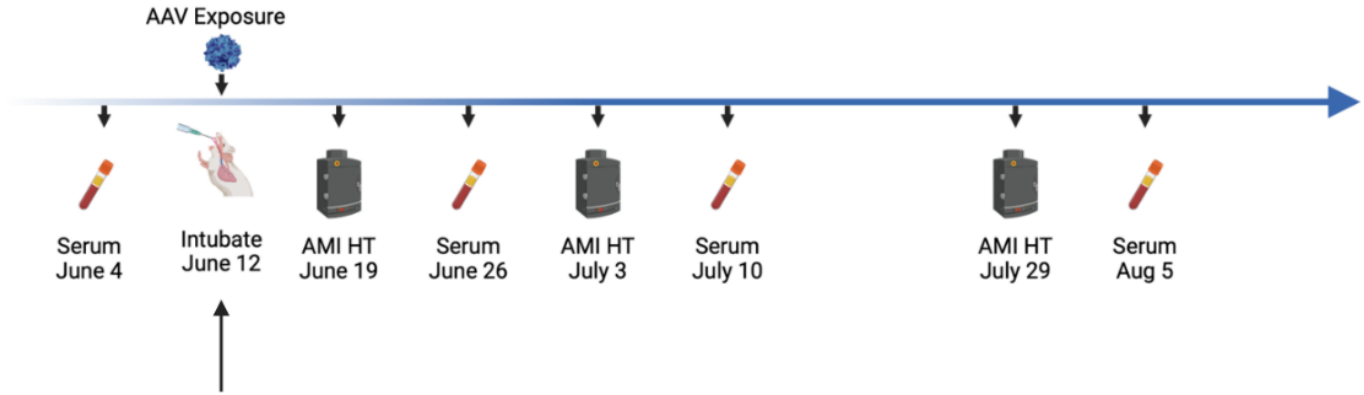


Treatment Groups:

1. No Treatment n=3
2. AAV2-mCherry (USC Vector Core) n=2
3. AAV6-mCherry (USC Vector Core) n=2
4. AAV6.2FF-mCherry (Guelph/OHRI) n=2
5. AAV6.2FF-fLuciferase$_{TLR9i}$ (Guelph/OHRI) n=2


AMI-HT Imaging D7
No treatment-mCherry
AAV2-mCherry
AAV6-mCherry
AAV6.2FF-mCherry
No treatment-fLuc
AAV6.2FF-fLuc_TLR9i
AMI-HT Imaging D21
No Treatment - mCherry
AAV2-mCherry
AAV6-mCherry
AAV6.2FF-mCherry
No Treatment-fLuc
AAV6.2FF-fLuc_TLR9i

**B**

C

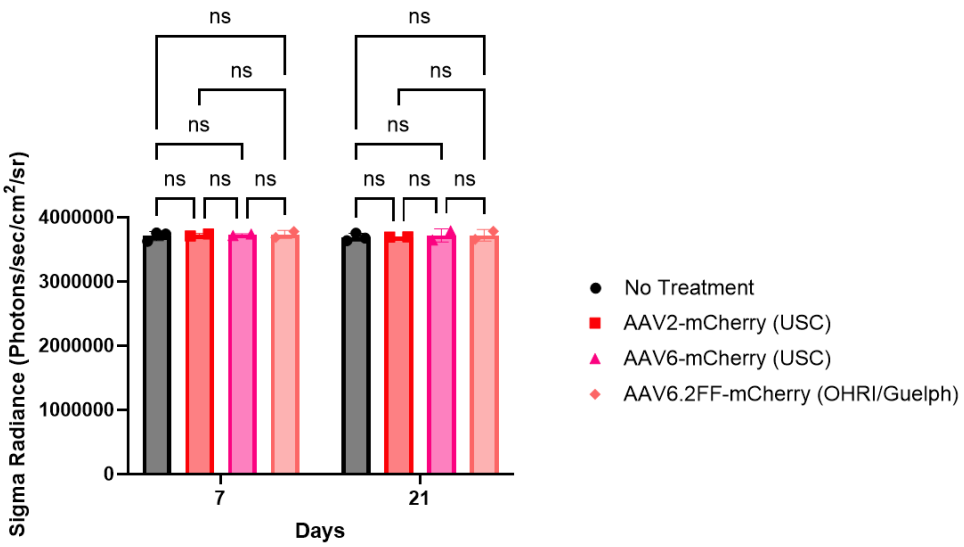
ns
ns
ns
ns ns ns
ns
ns
ns
ns ns ns
Sigma Radiance (Photons/sec/cm²/sr)
4000000
3000000
2000000
1000000
0
7
21
Days
No Treatment
AAV2-mCherry (USC)
AAV6-mCherry (USC)
AAV6.2FF-mCherry (OHRI/Guelph)

D

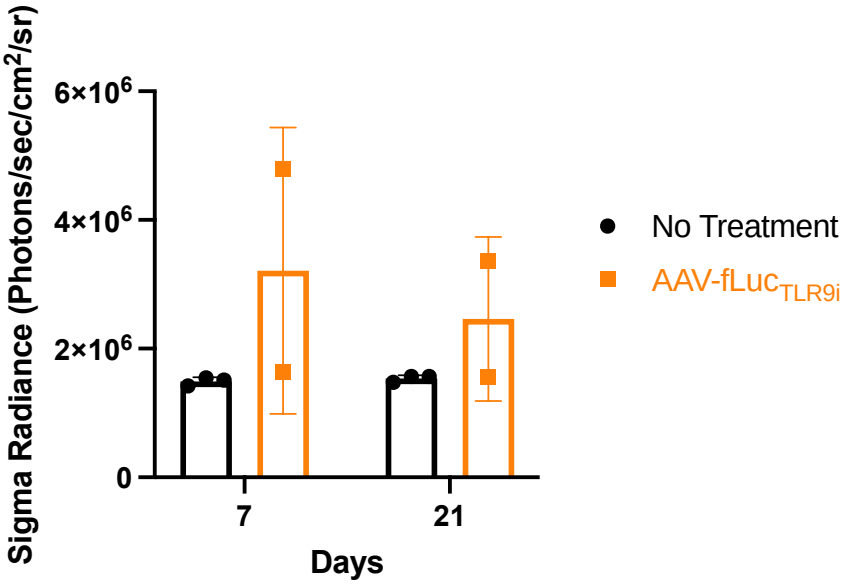
Sigma Radiance (Photons/sec/cm²/sr)
6×10⁶
4×10⁶
2×10⁶
0
7
21
Days
No Treatment
AAV-fLuc TLR9i

**E**

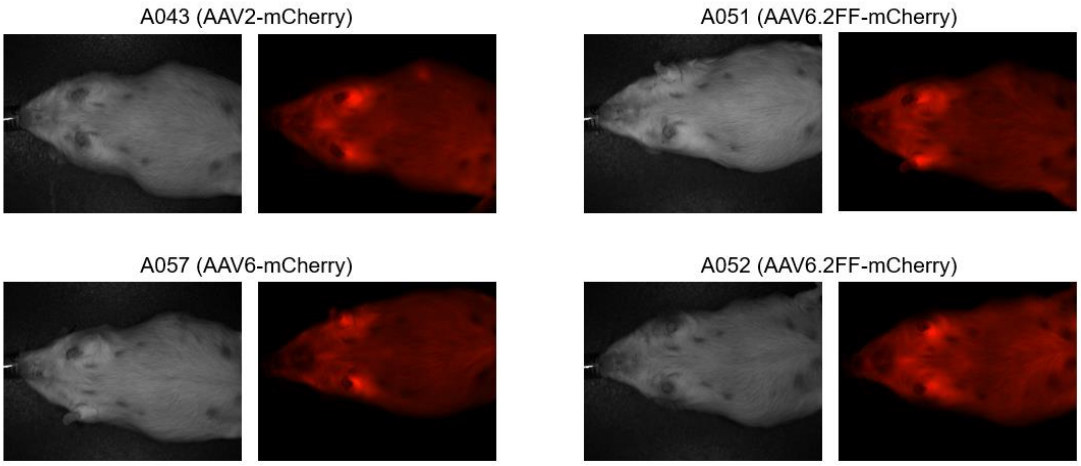


**Figure 6: AAV vector assessment study to determine variability in efficacy.**

(A) Timeline with 5 mouse groups (n=2 each group) with labeled points for serum collection and additional AMI HT in vivo imaging (B) AMI HT in vivo images of mice 7 and 21 days after AAV exposure. Fluorescence (mCherry) groups were imaged at 570 nm excitation and 630 nm emission at 5% excitation power. Bioluminescence (firefly luciferase) images were captured with D-Luciferan substrate injected subcutaneously 15-30 minutes prior to image capture on the Bioluminescence setting in Aura software. (C) Quantification of mCherry levels from D7 and D21 in sigma radiance (Photons/sec/cm$^2$/steradian). (D) Quantification of fLuciferase levels from D7 and D21 in sigma radiance (Photons/sec/cm$^2$/steradian). (E) MAESTRO imaging 16 days after AAV exposure to test for mCherry signal on mice with fur shaved in target region.

### *3.3 TLR9i sequences improve human SFTPB expression in repeat doses*

To further validate qPCR results that showed increased *SFTPB* expression with the addition of TLR9i sequences, immunoblotting was done using different anti-SP-B antibodies, one which recognizes the proSP-B form (Figure 7A), and one that is more targeted to the mature form of SP-B (Figure 7B-C). Higher intensity banding was seen in the proSP-B and mature SP-B blots with mice that received a vector with TLR9i sequences (Figure 7A-C).

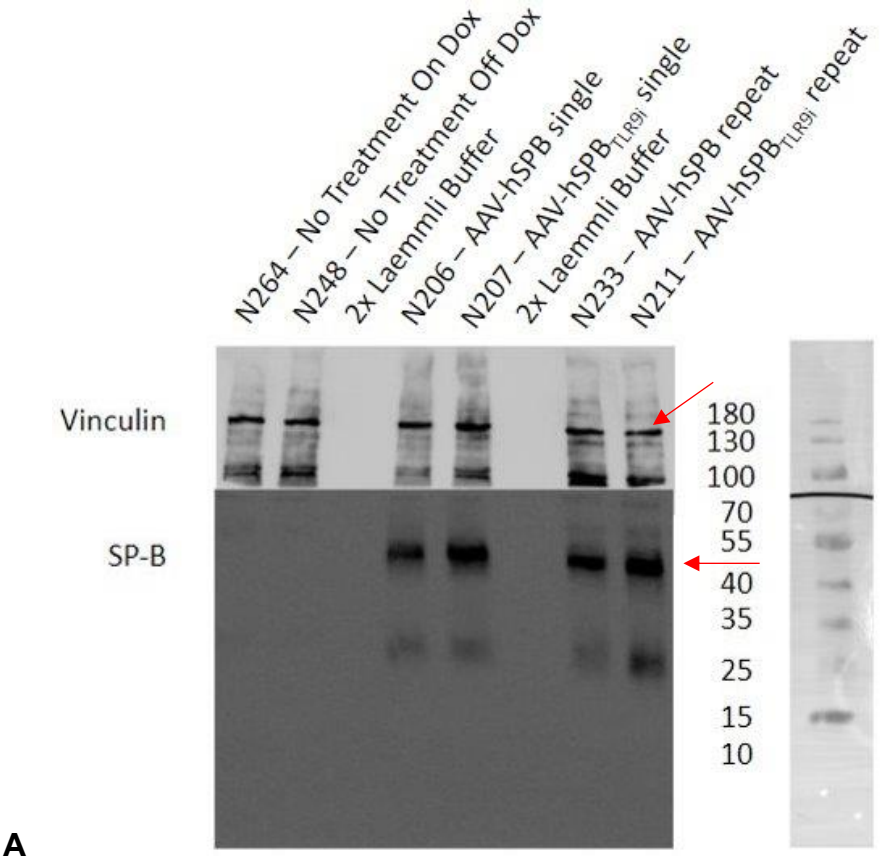
N264 – No Treatment On Dox
N248 – No Treatment Off Dox
2x Laemmli Buffer
N206 – AAV-hSPB single
N207 – AAV-hSPB$_{TLR9i}$ single
2x Laemmli Buffer
N233 – AAV-hSPB repeat
N211 – AAV-hSPB$_{TLR9i}$ repeat
Vinculin
SP-B
180
130
100
70
55
40
35
25
15
10

**A**

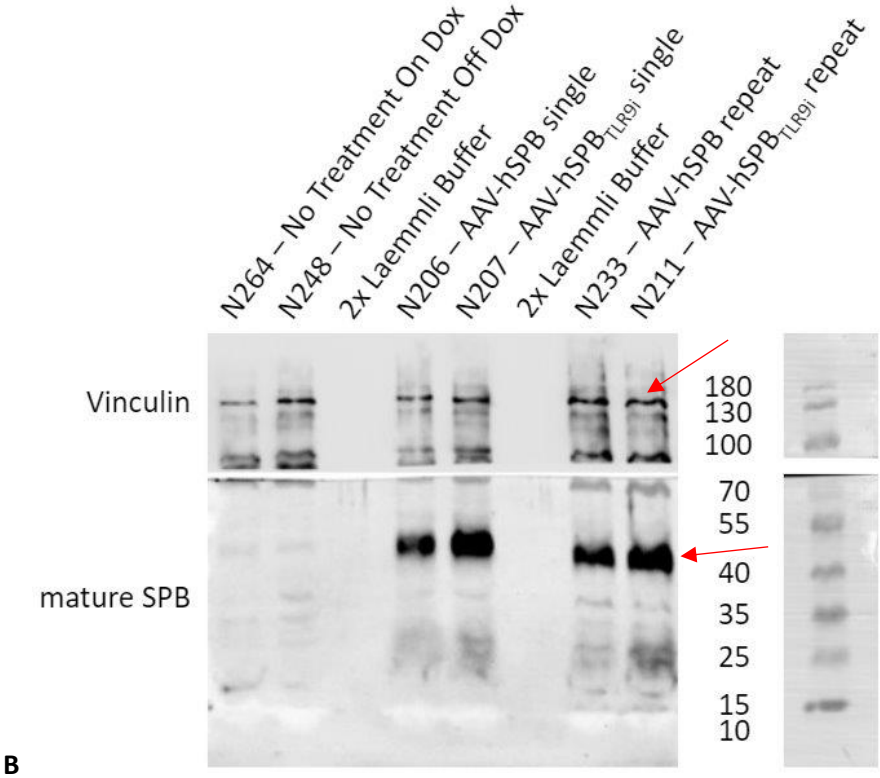
N264 – No Treatment On Dox
N248 – No Treatment Off Dox
2x Laemmli Buffer
N206 – AAV-hSPB single
N207 – AAV-hSPB$_{TLR9i}$ single
2x Laemmli Buffer
N233 – AAV-hSPB repeat
N211 – AAV-hSPB$_{TLR9i}$ repeat
Vinculin
mature SPB
180
130
100
70
55
40
35
25
15
10

**B**

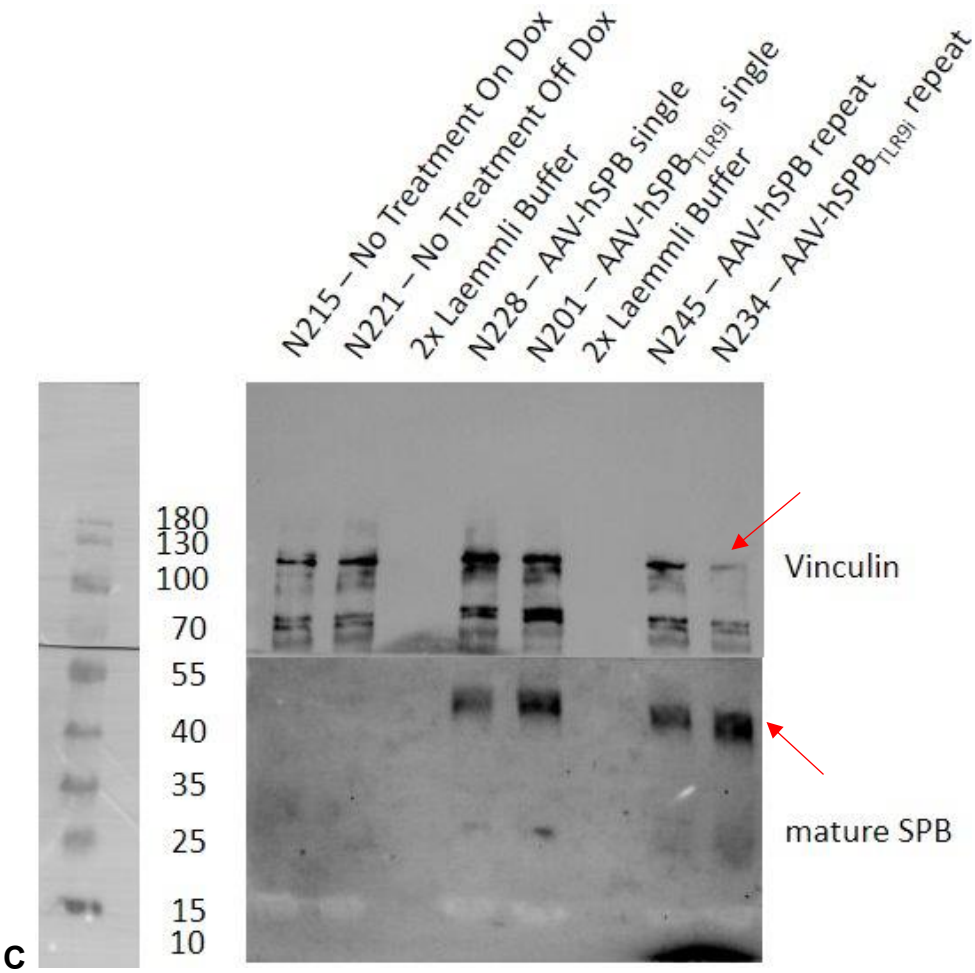


**Figure 7: Human SFTPB levels by immunoblotting of proSP-B and mature SP-B.**

(A) Western blot of pro SP-B and reference gene, Vinculin. (B) Western blot of mature SP-B and reference gene, Vinculin. (C) Western blot of mature SP-B and reference gene, Vinculin.

### *3.4 Gene Expression Analysis*

To better understand the impact on the immune response after AAV readministration, the lungs were analyzed 7 days after the second dose of either AAV-hSPB or AAV-hSPB$_{TLR9i}$ (Figure 8A). Analysis was performed using nCounter technology (NanoString) and a panel of 773 genes associated with the host immune and inflammatory response to measure detectable changes in these genes (Murine Host Response Panel). All gene expression changes were compared to the No Treatment (On Dox) group. All gene expression changes were controlled for false discovery rate and were represented by adjusted *P* values. Single doses of the gene therapy treatment with and without TLR9i sequences caused very little change to gene expression compared to the No Treatment (On Dox) group (Figure 9A-B) After a repeat dose of AAV-hSPB, there were 136 genes with a significant change in expression (Figure 10A). However, after a repeat dose of AAV-hSPB$_{TLR9i,}$ only 9 of the 773 genes had a significant change in expression levels (Figure 10B). The heatmap of undirected global significance scores show increased expression in pathways after a repeat dose of AAV-hSPB and less expression changes after a repeat dose of AAV-hSPB$_{TLR9i}$ (Figure 11A). nCounter software also provided the relative cell abundance numbers for T-helper 1 cells (Th1), which showed the highest count of Th1 cells after a repeat dose of AAV-hSPB, but a lower relative cell count after a repeat dose of AAV-hSPB$_{TLR9i}$ (Figure 12A). The marker used by the nCounter software for Th1 cells is a gene, *Tbx21* or T-bet, which is a gene that is responsible for the transcription factor T-box that is expressed in Th1 cells[17].

**A**

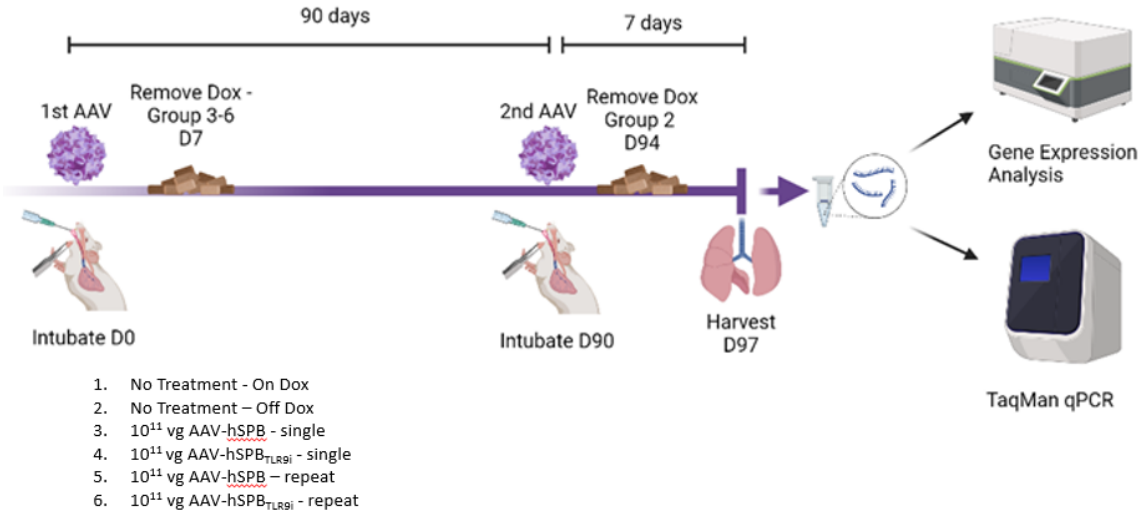


**Figure 8: Study timeline for gene expression analysis**

(A) Timeline of study where murine lungs were harvested 7 days after the second AAV dose for gene expression analysis

AAV-hSPB (single) n=4 vs No Treatment (On Dox) n=4: 97 Days

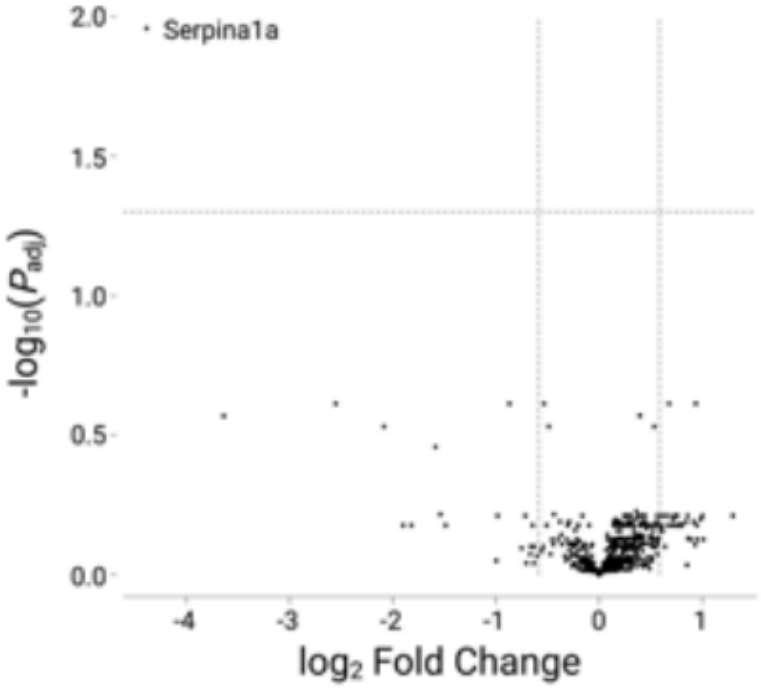


**A**

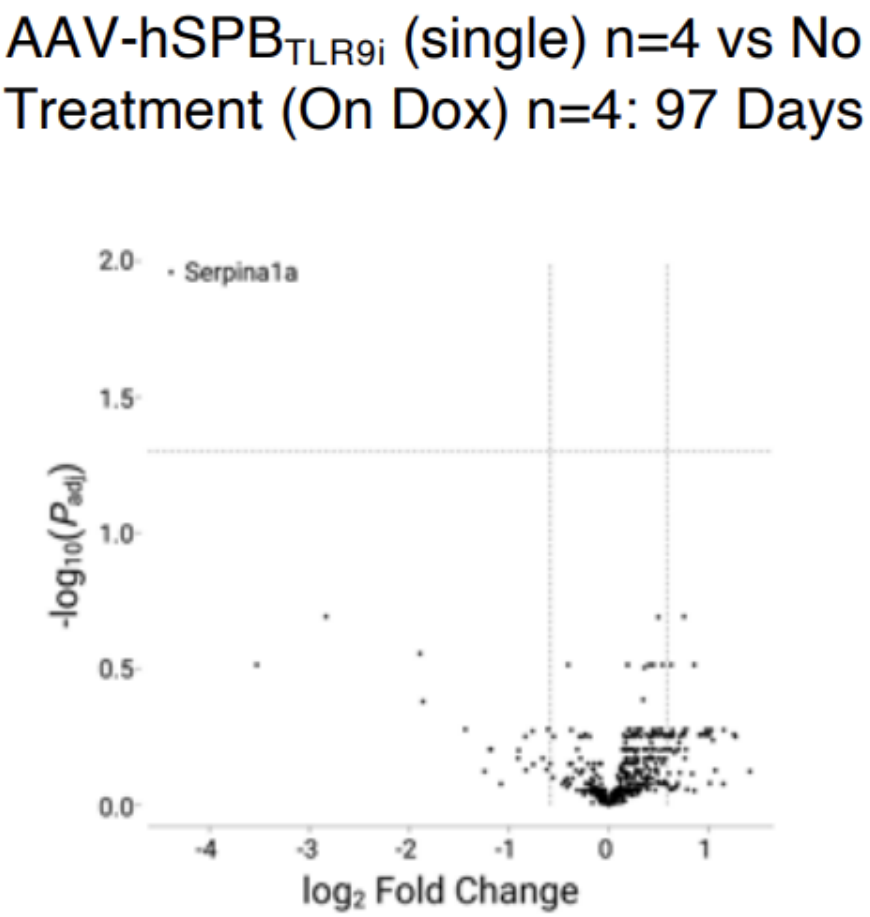


**B**

**Figure 9: Volcano plots show no gene expression changes after a single dose of AAV-hSPB with or without TLR9i**

(A) Volcano plot of AAV-hSPB single compared to No Treatment (On Dox). (B) Volcano plot of AAV-hSPB$_{TLR9i}$ single compared to No Treatment (On Dox).

# AAV-hSPB (repeat) n=4 vs No Treatment (On Dox) n=4: 97 Days

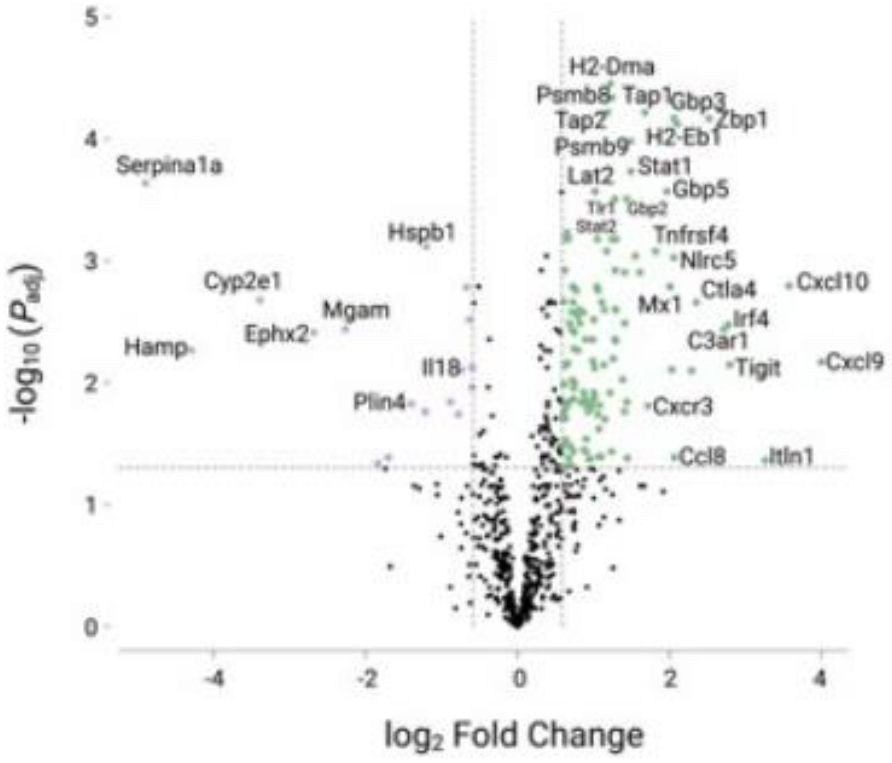


**A**

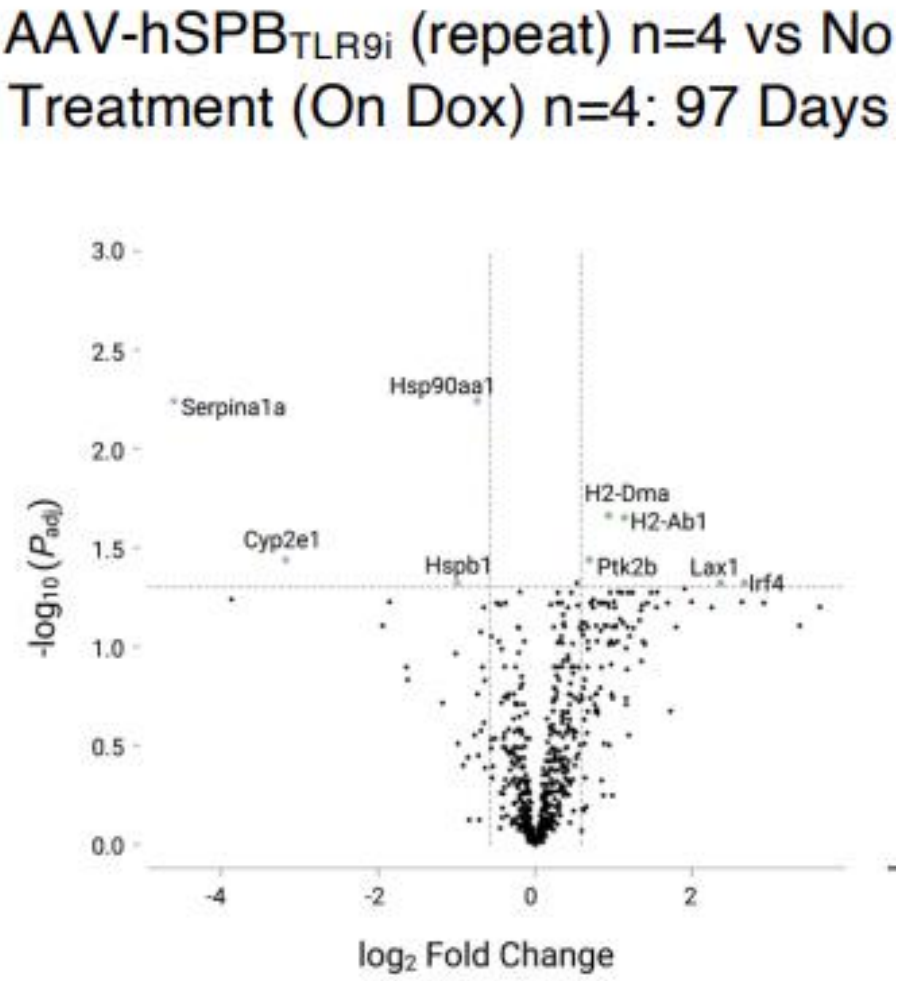


**B**

**Figure 10: Volcano plots show greatest gene expression changes with repeat dose of AAV-hSPB**

(A) Volcano plot of gene expression changes between AAV-hSPB (repeat) n=4 and No Treatment (On Dox) n=4. (B) Volcano plot of gene expression changes between AAV-hSPB$_{TLR9i}$ (repeat) n=4 and No Treatment (On Dox) n=4

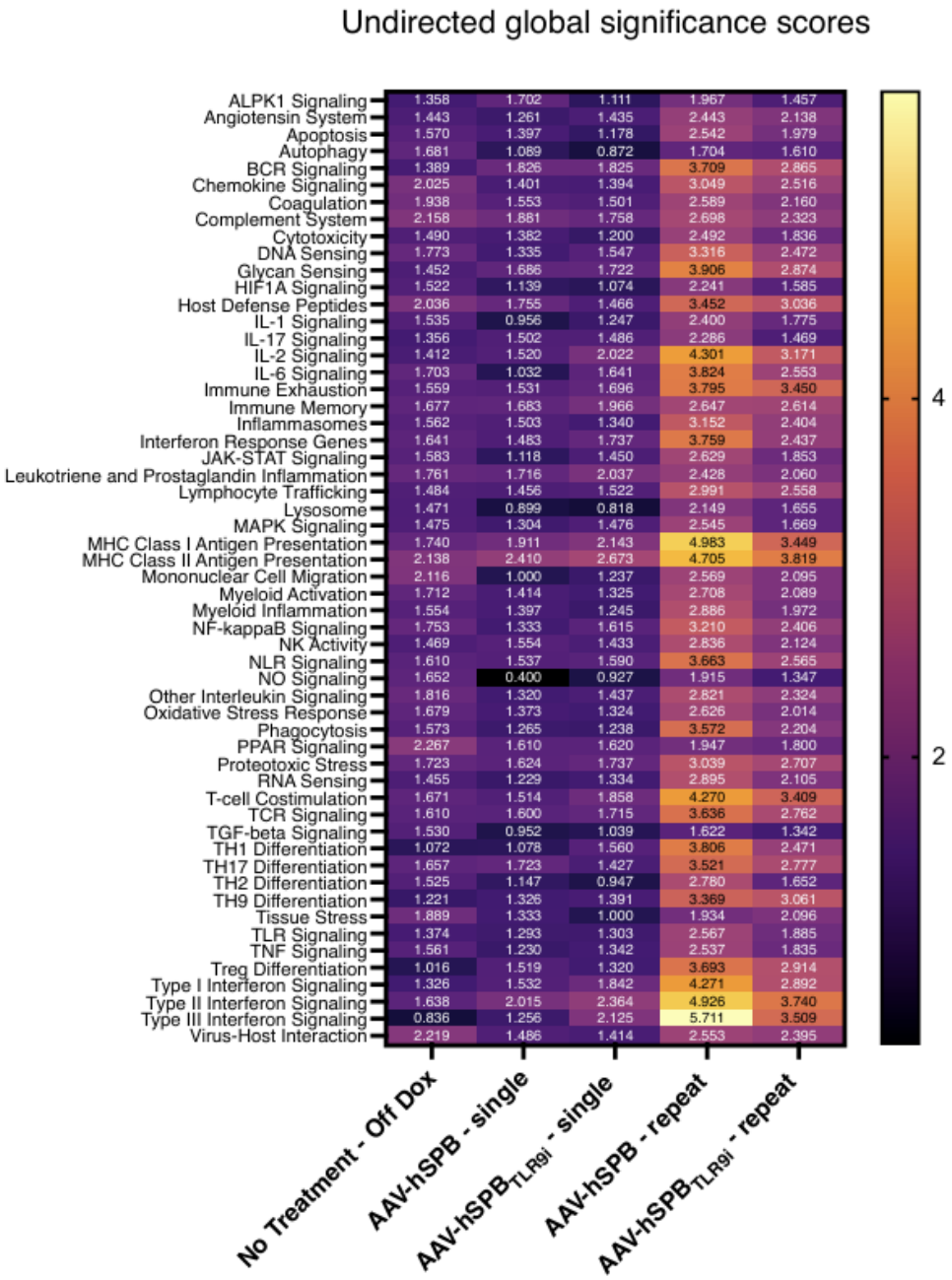


**A**

**Figure 11: Heatmap shows increased gene expression in interferon pathways after repeat dose of AAV-hSPB**

(A) Heatmap of undirected global significance scores where light yellow indicates increased gene expression changes and dark purple indicates less gene expression changes.

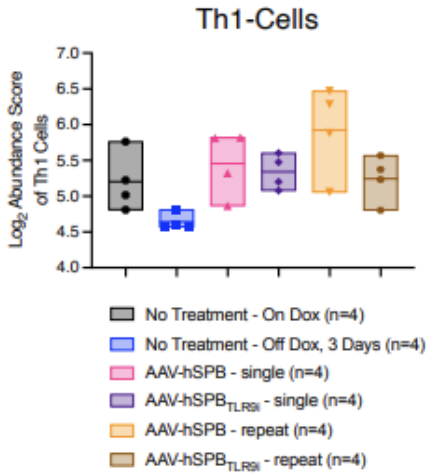


**A**

**Figure 12: Relative cell abundance of Th1 cells is greatest after a repeat dose of AAV-hSPB**

(A) Relative cell abundance levels of Th1 cells, where *Tbx21* is the marker used by nCounter to measure Th1 cell levels.

From these results, genes of interest were further assessed to validate critical genes directly affected by TLR9 inhibition. These included *Stat1* and *Mx1* which were both upregulated significantly between the No Treatment (on dox) and the AAV-hSPB repeat group (Figure 10A), but not between the No Treatment (on dox) and the AAV-hSPB$_{TLR9i}$ repeat group (Figure 10B). *Stat1* plays a key role in mediating the cellular response to different types of interferons, and *Mx1* plays an important role in the innate antiviral immune response[18, 19]. Other genes of interest that were assessed included *Cxcl10, Zbp1,* and *Serpina1a. Cxcl10* is an inflammatory chemokine that plays a role in mediating the immune response[20]. The *Zbp1* gene acts as an innate immune sensor which activates interferon (IFN)

1 and NF-κB signaling, both of which indicate its role in fighting pathogen invasion[21]. *Serpina1a* has been shown to have protective features over alveolar tissues and prevent proteolytic degradation as a result of the inflammatory response[22]. By nCounter analysis, *Cxcl10* and *Zbp1* were upregulated significantly after a repeat dose of AAV-hSPB, and *Serpina1a* was downregulated after a repeat dose of AAV-hSPB (Figure 10A).

### *3.5 Validation of Gene Expression Analysis*

To validate the gene expression analysis results by nCounter, reverse transcription qPCR (TaqMan) was performed on *Cxcl10, Zbp1, Serpina1a, Mx1, and Stat1*. Although the qPCR results demonstrated similar trends as the nCounter gene expression data, the qPCR results for *Cxcl10, Zbp1,* and *Serpina1a* did not demonstrate identical findings as gene expression analyses (Figure 13A). However, *Mx1* and *Stat1* did show a significant increase in expression between the No Treatment (On Dox) group and the AAV-hSPB repeat group (Figure 13B). In contrast, there was no notable change with the AAV-hSPB$_{TLR9i}$ group and No Treatment (On Dox) group (Figure 13B). These genes did replicate the nCounter findings and suggest they may have critical roles in allowing AAV redosing.

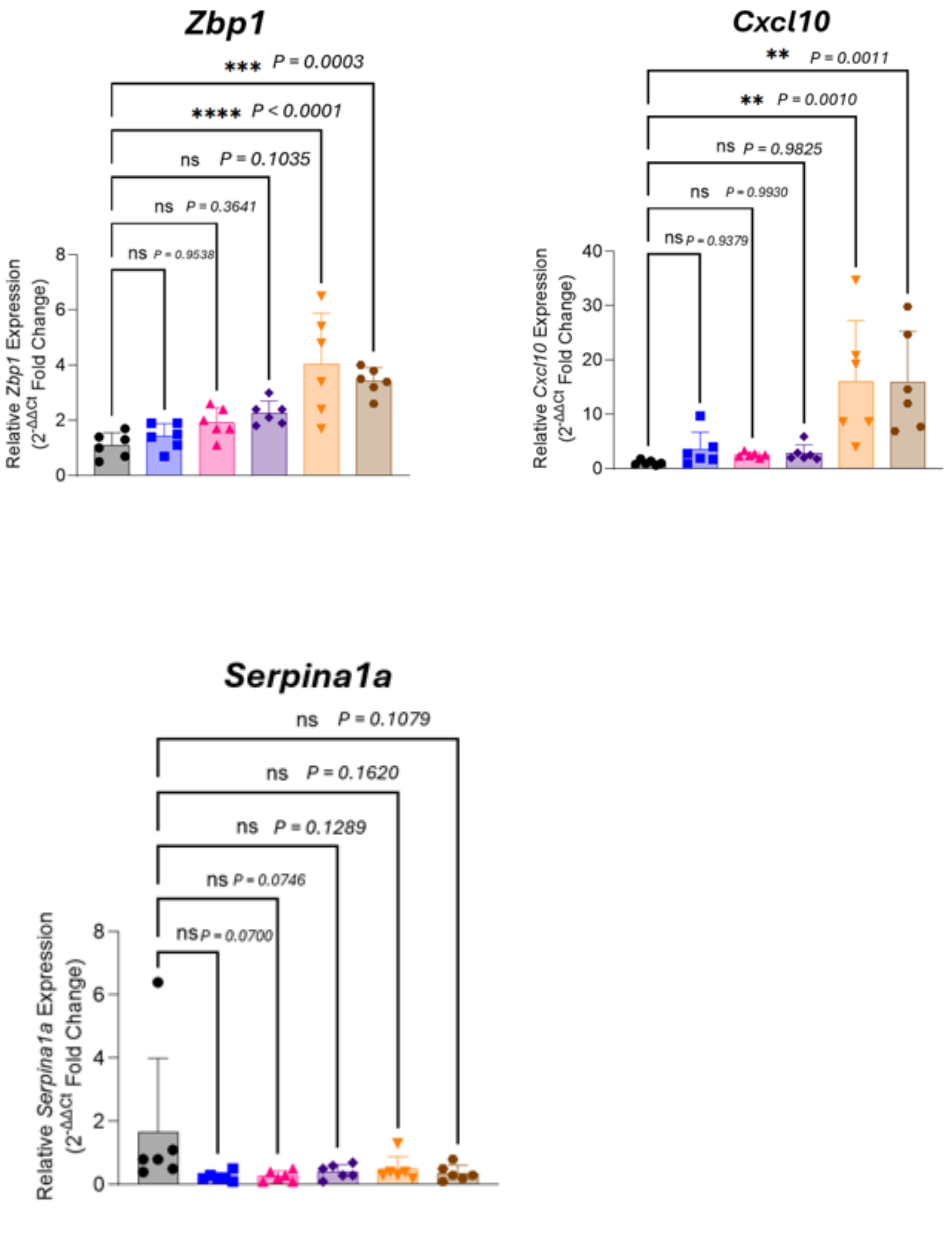
Zbp1
*** P = 0.0003
**** P < 0.0001
ns P = 0.1035
ns P = 0.3641
ns P = 0.9538
Relative Zbp1 Expression
(2-ΔΔCt Fold Change)
0
2
4
6
8
Cxcl10
** P = 0.0011
** P = 0.0010
ns P = 0.9825
ns P = 0.9930
ns P = 0.9379
Relative Cxcl10 Expression
(2-ΔΔCt Fold Change)
0
10
20
30
40
Serpina1a
ns P = 0.1079
ns P = 0.1620
ns P = 0.1289
ns P = 0.0746
ns P = 0.0700
Relative Serpina1a Expression
(2-ΔΔCt Fold Change)
0
2
4
6
8

**A**

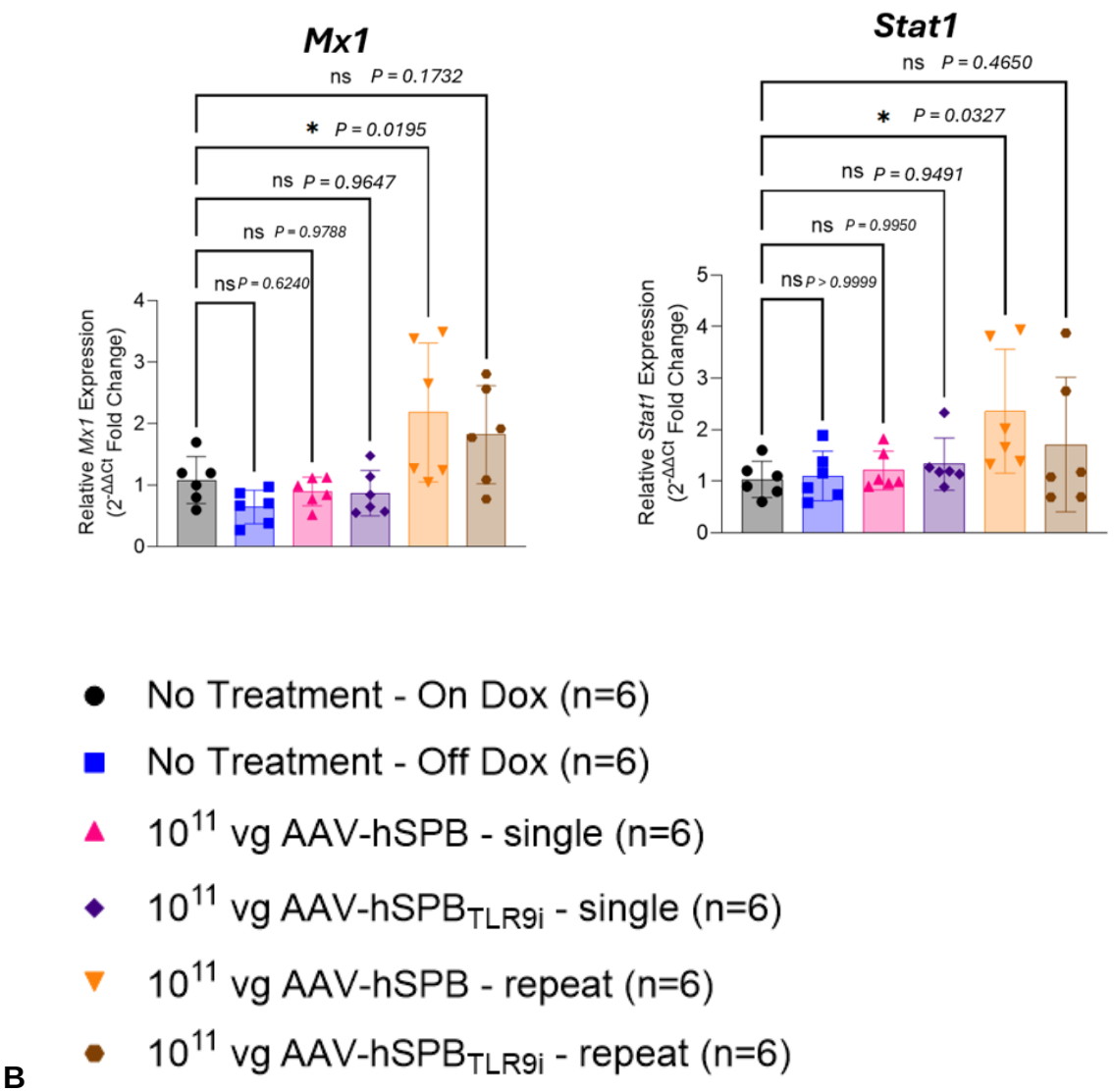


**B**

**Figure 13: Mx1 and Stat1 show significant differences between the no treatment (on dox) and AAV-hSPB repeat groups.**

(A) Gene expression changes of, *Zpb1, Cxcl10, Serpina1a* by reverse transcription rt-qPCR (p-values calculated by ordinary one-way ANOVA with Dunnett's multiple comparisons *post hoc* test, ns = not significant, *P<0.05) (B) Gene expression changes of *Mx1* and *Stat1* by reverse transcription rt-qPCR (p-

values calculated by ordinary one-way ANOVA with Dunnett's multiple comparisons *post hoc* test, ns = not significant, *P<0.05)

### *3.6 Validation of Stat1 by immunoblotting*

Expression levels were also further validated by immunoblotting. The Stat1 immunoblot results showed increased expression in the repeat AAV-hSPB lanes compared to the no treatment (on dox) group and a reduction in expression in mice with repeat AAV-hSPB$_{TLR9i}$, which further validates the qPCR results (Figure 14A-E). Quantification of Stat1 followed the trend seen by qPCR with increased expression following repeat doses of AAV-hSPB (Figure 14E).

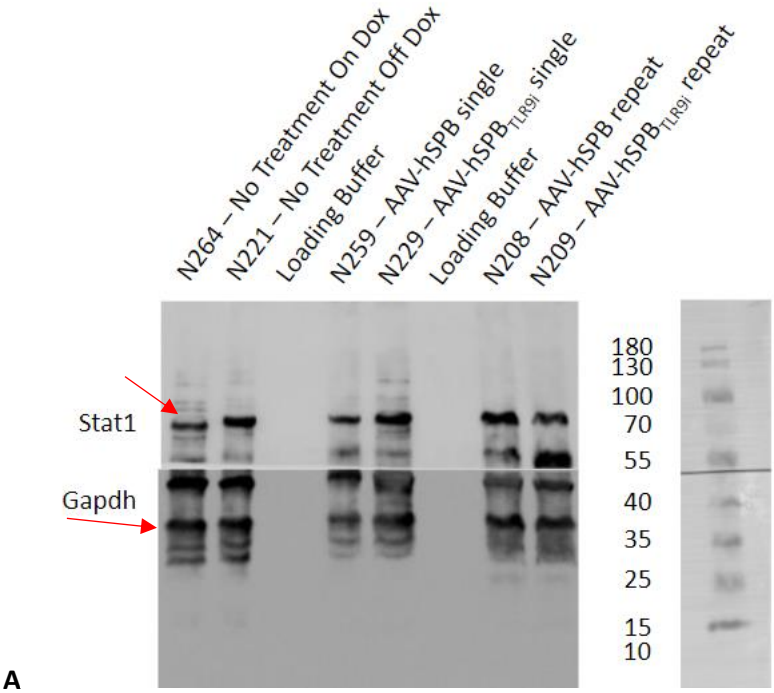
N264 – No Treatment On Dox
N221 – No Treatment Off Dox
Loading Buffer
N259 – AAV-hSPB single
N229 – AAV-hSPB$_{TLR9i}$ single
Loading Buffer
N208 – AAV-hSPB repeat
N209 – AAV-hSPB$_{TLR9i}$ repeat
Stat1
Gapdh
180
130
100
70
55
40
35
25
15
10

**A**

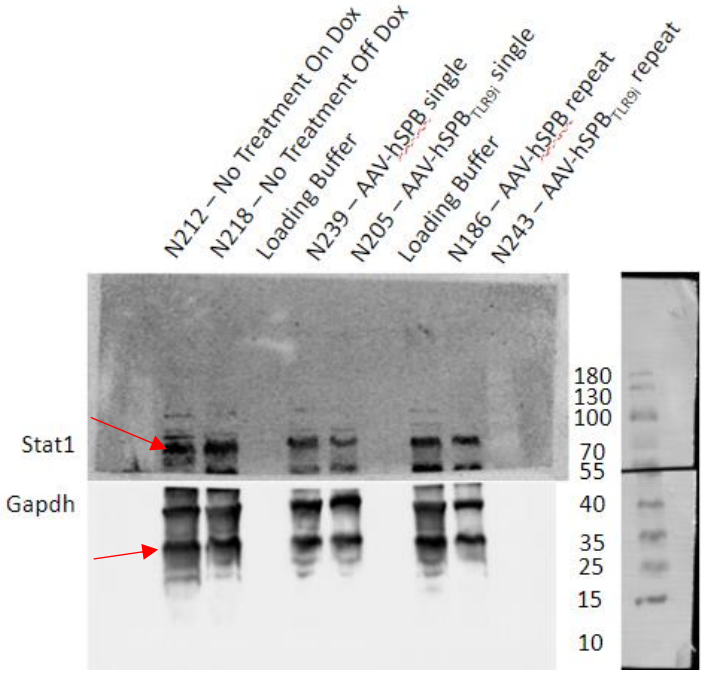
N212 – No Treatment On Dox
N218 – No Treatment Off Dox
Loading Buffer
N239 – AAV-hSPB single
N205 – AAV-hSPB$_{TLR9i}$ single
Loading Buffer
N186 – AAV-hSPB repeat
N243 – AAV-hSPB$_{TLR9i}$ repeat
Stat1
Gapdh
180
130
100
70
55
40
35
25
15
10

**B**

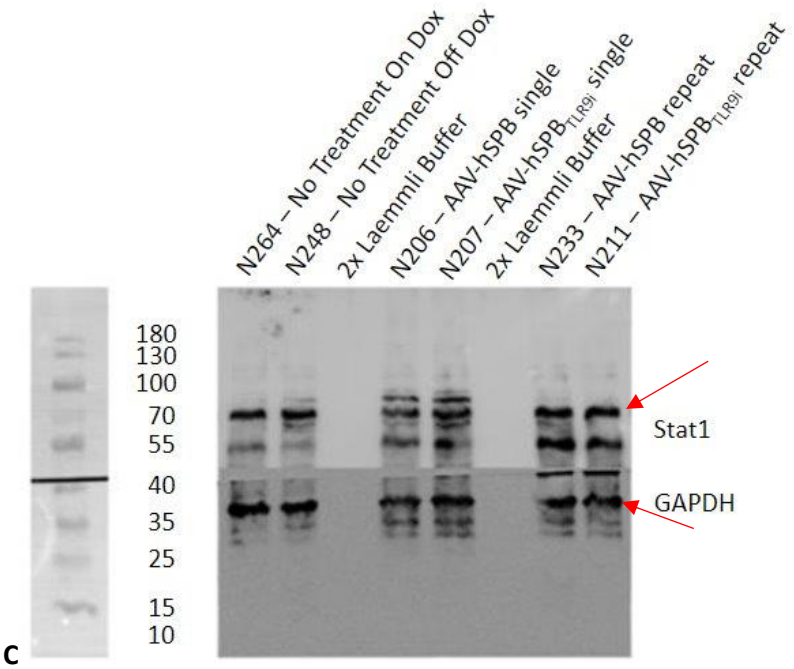
N264 – No Treatment On Dox
N248 – No Treatment Off Dox
2x Laemmli Buffer
N206 – AAV-hSPB single
N207 – AAV-hSPB$_{TLR9i}$ single
2x Laemmli Buffer
N233 – AAV-hSPB repeat
N211 – AAV-hSPB$_{TLR9i}$ repeat
180
130
100
70
55
40
35
25
15
10
Stat1
GAPDH

C

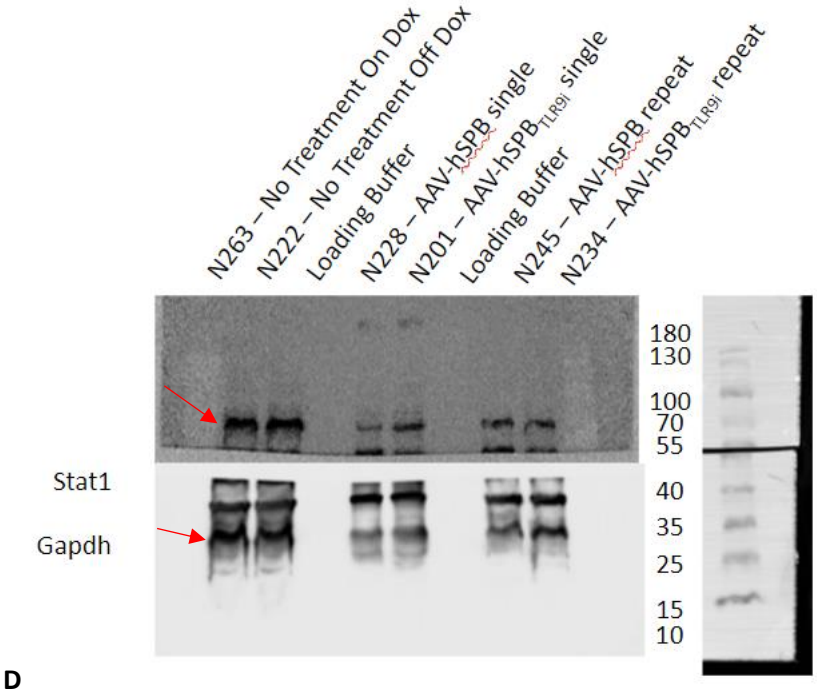
N263 – No Treatment On Dox
N222 – No Treatment Off Dox
Loading Buffer
N228 – AAV-hSPB single
N201 – AAV-hSPB$_{TLR9i}$ single
Loading Buffer
N245 – AAV-hSPB repeat
N234 – AAV-hSPB$_{TLR9i}$ repeat
180
130
100
70
55
40
35
25
15
10
Stat1
Gapdh

D

E

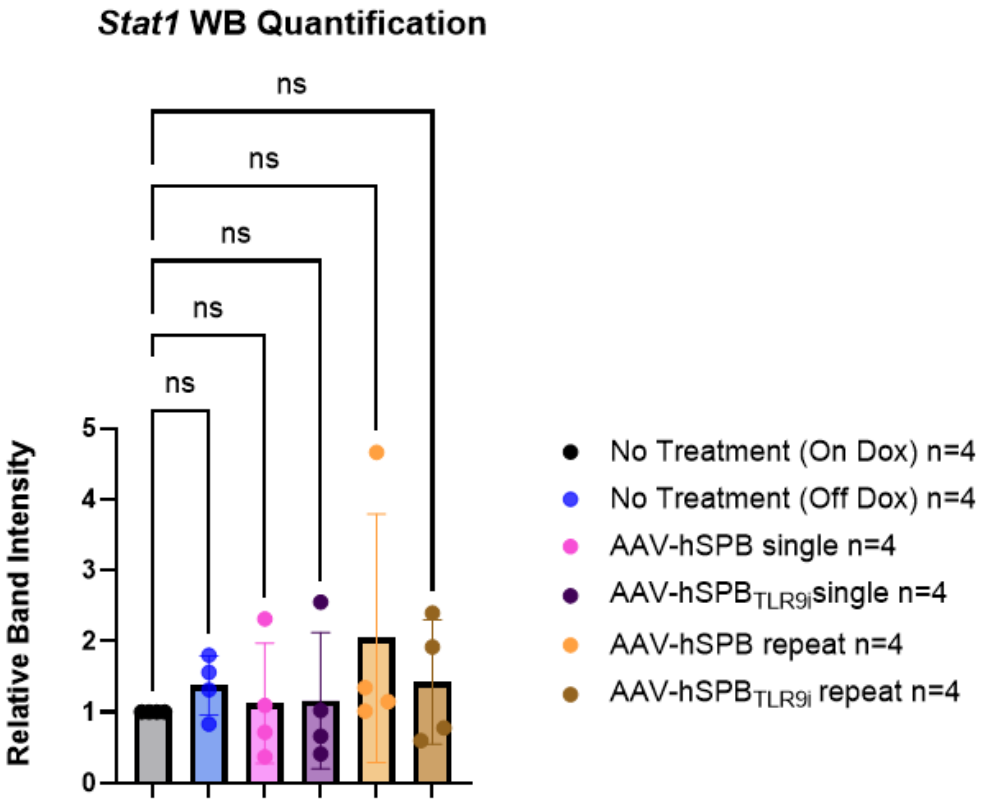


**Figure 14: Stat1 by immunoblotting validates qPCR and shows increased expression in AAV-hSPB repeat group.**

(A) Western blot of Stat1 with Gapdh as a reference gene. (B) Western blot of Stat1 with Gapdh as a reference gene. (C) Western blot of Stat1 with Gapdh as a reference gene. (D) Western blot of Stat1 with Gapdh as a reference gene. (E) Quantification of Stat1 western blots by ImageJ software.

### *3.7 Validation of Tbx21 by immunoblotting*

Increased *Tbx21* expression levels were observed with AAV-hSPB, and less with AAV-hSPB$_{TLR9i}$ (Figure 15A-B), but this was not observed consistently (Figure 15C). Quantification of the Tbx21 immunoblots showed an overall decrease in *Tbx21* gene expression based on relative band intensity of repeat AAV-hSPB$_{TLR9i}$ and an increase in gene expression with repeat doses of AAV-hSPB confirming the cell profiling results from nCounter (Figure 15D).

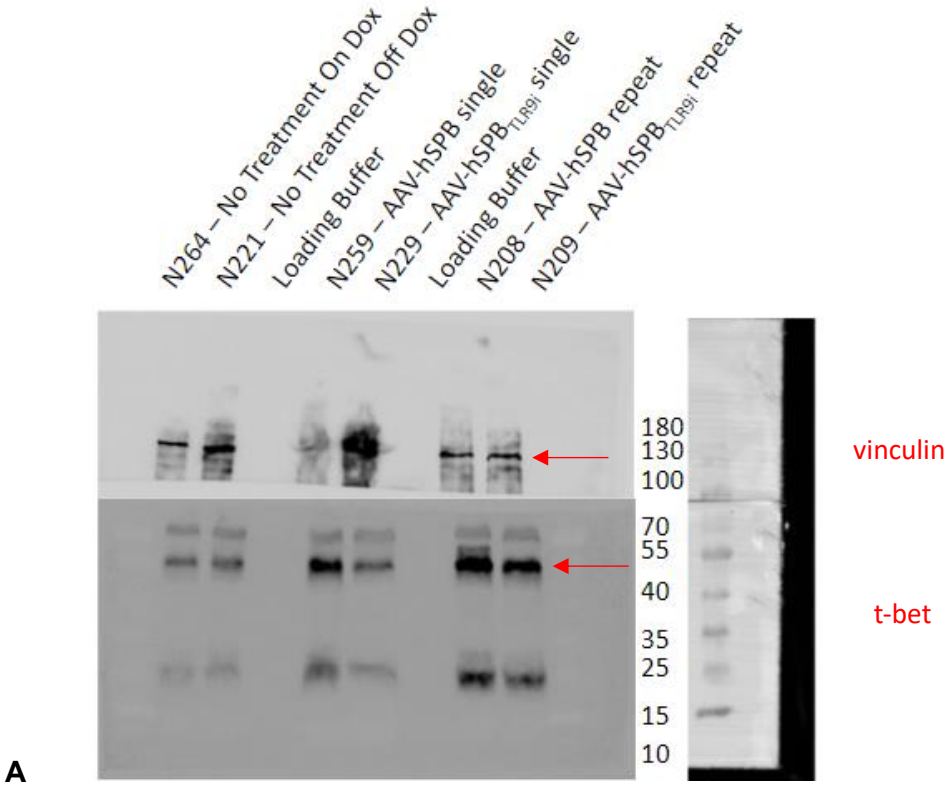
N264 – No Treatment On Dox
N221 – No Treatment Off Dox
Loading Buffer
N259 – AAV-hSPB single
N229 – AAV-hSPB$_{TLR9i}$ single
Loading Buffer
N208 – AAV-hSPB repeat
N209 – AAV-hSPB$_{TLR9i}$ repeat
180
130
100
70
55
40
35
25
15
10
vinculin
t-bet

A

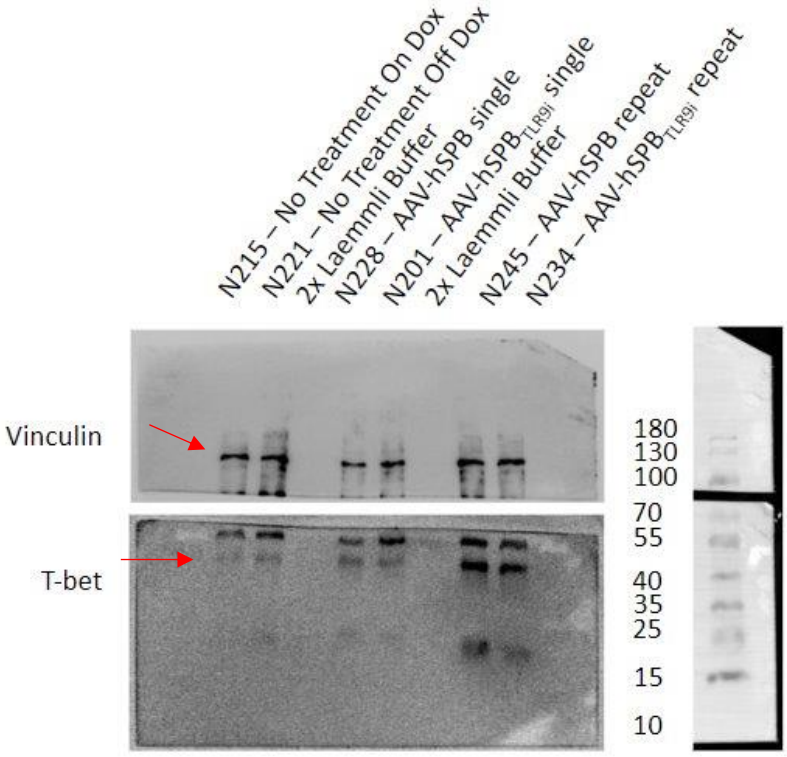
N215 – No Treatment On Dox
N221 – No Treatment Off Dox
2x Laemmli Buffer
N228 – AAV-hSPB single
N201 – AAV-hSPB$_{TLR9i}$ single
2x Laemmli Buffer
N245 – AAV-hSPB repeat
N234 – AAV-hSPB$_{TLR9i}$ repeat
Vinculin
T-bet
180
130
100
70
55
40
35
25
15
10

B

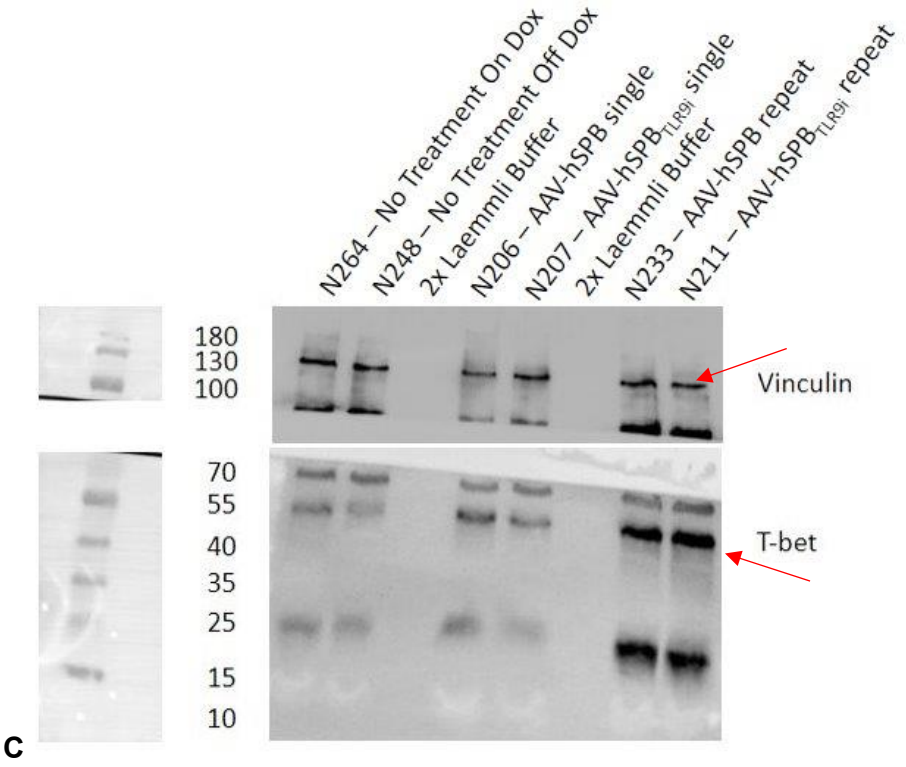


C

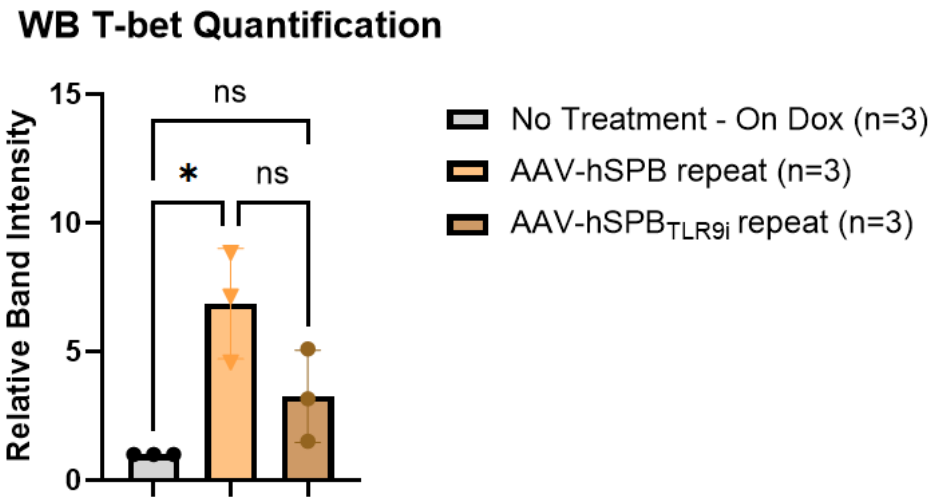


D

**Figure 15: Immunoblotting of Tbx21 confirms cell profiling of Th1 cells**

(A) Western blot of T-bet with Vinculin as a reference gene. (B) Western blot of T-bet with Vinculin as a reference gene. (C) Western blot of T-bet with Vinculin as

a reference gene. (D) The quantification of the 3 T-bet western blots (n=3) by ImageJ software.

## *4.0 Discussion*

### *4.1 Assessment of AAV Vector Efficacy*

After an initial attempt to determine if pre-existing immunity could be overcome by utilizing the TLR9i sequences, it was found that the potency of the AAV6-mCherry vectors was minimal after administration to the mice. When serum antibody levels were measured it was found that neither of the mice had antibodies against AAV6 (Figure 2B). We deduced that this inhibition was likely due to the vector titers of purified AAV6 received from the USC Viral Vector Core were not sufficient. Original titers that were received from the USC Viral Vector Core were AAV2-mCherry ($2.12 \times 10^{15}$ TU/mL), and AAV6-mCherry ($1.76 \times 10^{15}$ TU/mL). The dose delivered to the mice was $1 \times 10^{11}$ TU/mouse for both vectors. Since there was a reporter gene attached to the vector, we further measured levels of mCherry by AMI-HT *in vivo* imaging and found that there were minimal amounts of fluorescence in mice (Figure 2C) indicating the imaging apparatus was likely not sensitive to fluorescence. These mice were further used to test the AAV-hSPB and AAV-hSPB$_{TLR9i}$ vectors from the USC Viral Vector Core at a higher dose of $1 \times 10^{12}$ TU/mouse. While the vectors did work the survival timelines were not as expected, which could be the result of using older mice, so this study needs to be repeated in a younger cohort of mice.

Further assessment of the vectors was performed to determine which were most effective at delivering the transgene. We generated a vector assessment study with 5 groups: no treatment, AAV2-mCherry, AAV6-mCherry, AAV6.2FF-mCherry, and AAV6.2FF-fLuc$_{TLR9i.}$ In vivo imaging 7 days after administration showed no fluorescence signal for all mCherry vectors, and only minimal signal was observed in the right lung of a mouse from the bioluminescence group (Figure 7B). Quantification of mCherry and fLuciferase show no discernable signal changes for mCherry, and decreased fLuciferase expression after the 7-day timepoint (Figure 7C-D). MAESTRO imaging was another method of visualizing mCherry that confirmed observations of AMI-HT imaging in that there was negligible mCherry signal (Figure 7E). To increase the potential for signal capture, the thorax region of the mice was shaved for MAESTRO and Day 21 AMI-HT imaging; however, there was still no signal. The likely reason for this is that imaging fluorescence with the AMI-HT in vivo imager is not sensitive to fluorescence since bioluminescence was observed with the AAV6.2FF-fLUC, but not the AAV6.2FF-mCherry.

### *4.2 Gene Expression Analysis*

The aim was to test the hypothesis that certain genes involved in the TLR9-dependent pathways were involved in the suppression of the immune response in mice that received AAV treatment with TLR9i sequences. While the incorporation of the TLR9i sequences improves survival in the SP-B deficient mice, there is still no means of confirming that the TLR9 pathway has been

inhibited when treated with AAV vectors. By analysis with the gene expression data, we were able to take a closer look at the impact on the immune system with either AAV-hSPB or AAV-hSPB$_{TLR9i}$.

We identified multiple genes and gene pathways that were involved in the host response to AAV. After repeat doses of AAV-hSPB$_{TLR9i}$ many genes, including genes involved in the interferon response pathways and Th1 cells, were not significantly changed compared to repeat doses of AAV-hSPB.

We validated a few of these genes by alternative methods including qPCR (*Stat1, Mx1*), as well as immunoblotting *(Stat1*). However, other genes (*Zbp1, Cxcl10, Serpina1a*) did not correspond to the nCounter data by qPCR. This suggests that *Stat1* or *Mx1* may be robust markers to demonstrate that TLR9 inhibition is occurring.

### *5.0 Conclusions and Future Directions*

Ultimately, this work demonstrates that there are immune response genes involved in the interferon response that are suppressed as a result of TLR9 inhibition through multiple validation methods. Initially, what began as an experiment to test if these TLR9 inhibitory sequences could overcome pre-existing immunity to AAV6 led us into a vector assessment study. The survival study using AAV-hSPB and AAV-hSPB$_{TLR9i}$ from the USC Vector Core demonstrated the vectors are potent but not to the level as previously observed with vectors produced from other facilities. However, confounding variables such

as the age of the mice, vector concentration, and the previous exposure they were subjected to prior to receiving a gene therapy dose could have played a role in why the mice did not survive as long. If vector concentration from the USC Viral Vector Core was overestimated, then by increasing the vector dosage administered to the mice there might be improved survival similar to previously established results.

Future directions for this work should focus on exploring other genes potentially involved with TLR9 inhibition. The ability to show TLR9 inhibition happening through a biomarker(s) has not been established and could have even broader applications than just the gene therapy field.

In terms of neonates with SP-B deficiency, access to a gene therapy treatment containing TLR9i sequences could permit serial administration in a clinical setting while these patients are intubated.

Additionally, these TLR9i sequences could be incorporated with other AAV-based gene therapy treatments to allow for readministration. The ability to readminister could expand the inclusion criteria for patients in clinical trials that were previously ineligible due to pre-existing immunity.

## *6.0 References*

(1) Whitsett, J. A.; Wert, S. E.; Weaver, T. E. Alveolar surfactant homeostasis and the pathogenesis of pulmonary disease. *Annu Rev Med* **2010**, *61*, 105-119. DOI: 10.1146/annurev.med.60.041807.123500 From NLM Medline.

(2) Han, S.; Mallampalli, R. K. The Role of Surfactant in Lung Disease and Host Defense against Pulmonary Infections. *Ann Am Thorac Soc* **2015**, *12* (5), 765-774. DOI: 10.1513/AnnalsATS.201411-507FR From NLM Medline.

(3) Hamvas, A.; Nogee, L. M.; Mallory, G. B., Jr.; Spray, T. L.; Huddleston, C. B.; August, A.; Dehner, L. P.; deMello, D. E.; Moxley, M.; Nelson, R.; et al. Lung transplantation for treatment of infants with surfactant protein B deficiency. *J Pediatr* **1997**, *130* (2), 231-239. DOI: 10.1016/s0022-3476(97)70348-2 From NLM Medline.

(4) Naso, M. F.; Tomkowicz, B.; Perry, W. L., 3rd; Strohl, W. R. Adeno-Associated Virus (AAV) as a Vector for Gene Therapy. *BioDrugs* **2017**, *31* (4), 317-334. DOI: 10.1007/s40259-017-0234-5 From NLM Medline.

(5) Hastie, E.; Samulski, R. J. Adeno-associated virus at 50: a golden anniversary of discovery, research, and gene therapy success--a personal perspective. *Hum Gene Ther* **2015**, *26* (5), 257-265. DOI: 10.1089/hum.2015.025 From NLM Medline.

(6) Geiger, J.; Aneja, M. K.; Rudolph, C. Vectors for pulmonary gene therapy. *Int J Pharm* **2010**, *390* (1), 84-88. DOI: 10.1016/j.ijpharm.2009.10.010 From NLM Medline.

(7) Kang, M. H.; van Lieshout, L. P.; Xu, L.; Domm, J. M.; Vadivel, A.; Renesme, L.; Muhlfeld, C.; Hurskainen, M.; Mizikova, I.; Pei, Y.; et al. A lung tropic AAV vector improves survival in a mouse model of surfactant B deficiency. *Nat Commun* **2020**, *11* (1), 3929. DOI: 10.1038/s41467-020-17577-8 From NLM Medline.

(8) Ronzitti, G.; Gross, D. A.; Mingozzi, F. Human Immune Responses to Adeno-Associated Virus (AAV) Vectors. *Front Immunol* **2020**, *11*, 670. DOI: 10.3389/fimmu.2020.00670 From NLM Medline.

(9) Rogers, G. L.; Martino, A. T.; Aslanidi, G. V.; Jayandharan, G. R.; Srivastava, A.; Herzog, R. W. Innate Immune Responses to AAV Vectors. *Front Microbiol* **2011**, *2*, 194. DOI: 10.3389/fmicb.2011.00194 From NLM PubMed-not-MEDLINE.

(10) Nidetz, N. F.; McGee, M. C.; Tse, L. V.; Li, C.; Cong, L.; Li, Y.; Huang, W. Adeno-associated viral vector-mediated immune responses: Understanding barriers to gene delivery. *Pharmacol Ther* **2020**, *207*, 107453. DOI: 10.1016/j.pharmthera.2019.107453 From NLM Medline.

(11) Chan, Y. K.; Wang, S. K.; Chu, C. J.; Copland, D. A.; Letizia, A. J.; Costa Verdera, H.; Chiang, J. J.; Sethi, M.; Wang, M. K.; Neidermyer, W. J., Jr.; et al. Engineering adeno-associated viral vectors to evade innate immune and inflammatory responses. *Sci Transl Med* **2021**, *13* (580). DOI: 10.1126/scitranslmed.abd3438 From NLM Medline.

(12) Kang, M. H. Novel Immune Response Evasion Strategy to Redose Adeno-Associated Viral Vectors and

Prolong Survival in Surfactant Protein-B Deficient Mice. Manuscript submitted for publication, 2024.

(13) Kang MH#, T. S., Westley C, Blouin T, Xu L, Chan YK, Lisk E, Vadivel A, Nangle K, Ramamurthy J, Pei Y, Allen S, Chiang JJ, Romeo MJ, Vaena S, O'Quinn EC, Nietert PJ, Church GM, Whitesett JA, Wootton SK, Thébaud B. Novel Immune Response Evasion Strategy to Redose Adeno-Associated Viral Vectors and

Prolong Survival in Surfactant Protein-B Deficient Mice. *Manuscript submitted to American Journal of Respiratory Cell and Molecular Biology*.

(14) Melton, K. R.; Nesslein, L. L.; Ikegami, M.; Tichelaar, J. W.; Clark, J. C.; Whitsett, J. A.; Weaver, T. E. SP-B deficiency causes respiratory failure in adult mice. *Am J Physiol Lung Cell Mol Physiol* **2003**, *285* (3), L543-549. DOI: 10.1152/ajplung.00011.2003 From NLM Medline.

(15) Kang MH#, T. S., Westley C, Blouin T, Xu L, Chan YK, Lisk E, Vadivel A, Nangle K, Ramamurthy J, Pei Y, Allen S, Chiang JJ, Romeo MJ, Vaena S, O'Quinn EC, Nietert PJ, Church GM, Whitesett JA, Wootton SK, Thébaud B. Redosing Adeno-associated viral vectors Containing TLR9 Inhibitory Oligonucleotides Prolongs Survival in Surfactant Deficient Mice. *Manuscript submitted to Science Translational Medicine.*

(16) Kang MH#, T. S., Westley C, Blouin T, Xu L, Chan YK, Lisk E, Vadivel A, Nangle K, Ramamurthy J, Pei Y, Allen S, Chiang JJ, Romeo MJ, Vaena S, O'Quinn EC, Nietert PJ, Church GM, Whitesett JA, Wootton SK, Thébaud B. Redosing Adeno-associated viral vectors Containing TLR9 Inhibitory Oligonucleotides Prolongs Survival in Surfactant Deficient Mice. . *Manuscript submitted to Science Translational Medicine*.

(17) Stolarczyk, E.; Lord, G. M.; Howard, J. K. The immune cell transcription factor T-bet: A novel metabolic regulator. *Adipocyte* **2014**, *3* (1), 58-62. DOI: 10.4161/adip.26220 From NLM PubMed-not-MEDLINE.

(18) Spitaels, J.; Van Hoecke, L.; Roose, K.; Kochs, G.; Saelens, X. Mx1 in Hematopoietic Cells Protects against Thogoto Virus Infection. *J Virol* **2019**, *93* (15). DOI: 10.1128/JVI.00193-19 From NLM Medline.

(19) Tolomeo, M.; Cavalli, A.; Cascio, A. STAT1 and Its Crucial Role in the Control of Viral Infections. *Int J Mol Sci* **2022**, *23* (8). DOI: 10.3390/ijms23084095 From NLM Medline.

(20) Liu, M.; Guo, S.; Stiles, J. K. The emerging role of CXCL10 in cancer (Review). *Oncol Lett* **2011**, *2* (4), 583-589. DOI: 10.3892/ol.2011.300 From NLM PubMed-not-MEDLINE.

(21) Hao, Y.; Yang, B.; Yang, J.; Shi, X.; Yang, X.; Zhang, D.; Zhao, D.; Yan, W.; Chen, L.; Zheng, H.; et al. ZBP1: A Powerful Innate Immune Sensor and Double-Edged Sword in Host Immunity. *Int J Mol Sci* **2022**, *23* (18). DOI: 10.3390/ijms231810224 From NLM Medline.

(22) Connolly, B.; Isaacs, C.; Cheng, L.; Asrani, K. H.; Subramanian, R. R. SERPINA1 mRNA as a Treatment for Alpha-1 Antitrypsin Deficiency. *J Nucleic Acids* **2018**, *2018*, 8247935. DOI: 10.1155/2018/8247935 From NLM PubMed-not-MEDLINE.